RAPHAELLE CROTEAU

70136

Flood Vulnerability Under Sea Level Rise for a Coastal Community Located in a Backbarrier Environment

UAlg FCT
UNIVERSIDADE DO ALGARVE
FACULDADE DE CIÊNCIAS E TECNOLOGIA

2022

RAPHAELLE CROTEAU

70136

Flood Vulnerability Under Sea Level Rise for a Coastal Community Located in a Backbarrier Environment

Master of Marine and Coastal Systems (MaCS)

Under the supervision of

André Pacheco and Óscar Ferreira (CIMA)

UAlg FCT
UNIVERSIDADE DO ALGARVE
FACULDADE DE CIÊNCIAS E TECNOLOGIA

2022

Declaration of Authorship of Work

Flood Vulnerability Under Sea Level Rise for a Coastal Community Located in a Backbarrier Environment

I, Raphaelle Croteau, declare I am the author of this work, which is original and unpublished. The sources consulted have been duly cited in the text and included in the list of references.

Raphaelle Croteau

Abstract

Sea level rise and other hydro-meteorological hazards will be the biggest threat to coastal communities within this century. In addition, coasts of the world have been highly modified to accommodate humans, which has caused numerous problems such as coastal erosion, pollution, and destruction of natural environments. Floods represent some of the most serious hazards on coastal areas. Their impact will most probably increase in the future due to both sea level rise and increased human occupation. The main objective of this study was to evaluate the potential ocean-driven inundation in a small village (Culatra, Portugal) located in a backbarrier environment, including the impacts of a recently built harbor and of sea level rise. The shoreline evolution was measured with the digital shoreline analysis system for a period of ~10 years before and after the harbor construction. Then, a flood analysis was performed using a new GIS based methodology to measure the inundation extension using total water levels (tides + storm surge + sea level rise) and an associated inundation extension. Finally, the post-harbor retreating trends were incorporated in the flood analysis to determine the influence of the harbor in the inundation extension. The results show that the shoreline changes related to the harbor construction are concentrated around the harbor, while the rest of the study area is stabilizing. The new inundation extension methodology shows that the village is somewhat protected for current and 2050 scenarios of total water levels of a 1-year return period but would be affected by 100-year return periods, especially in 2050. The shoreline retreat induced by the harbor shows minimal impacts in the flooding extension compared to the increase in water level. To prevent flooding in the next 30 years, simple measures like elevating dunes, nourishing key sectors, and protecting marsh vegetation can be very effective. For 2100, both scenarios (1-year and 100-year return periods) show a highly impacted village that will require strong adaptation measures in order to remain in the area after 2050 since all the main infrastructures would be flooded on a yearly basis.

Keywords: coastal hazards, inundation, coastal management, sea level rise, shoreline evolution

Sumário

A subida do nível do mar e outros riscos hidrometeorológicos serão a maior ameaça para as comunidades costeiras neste século. Além disso, as costas do mundo foram altamente modificadas para acomodar os humanos, o que causou numerosos problemas, tais como erosão costeira, poluição e destruição de ambientes naturais. As inundações representam alguns dos perigos mais graves nas zonas costeiras. O seu impacto irá muito provavelmente aumentar no futuro, devido tanto à subida do nível do mar como ao aumento da ocupação humana. O principal objectivo deste estudo foi avaliar a potencial inundação provocada pelos oceanos numa pequena aldeia (Culatra, Portugal) localizada num ambiente com obstáculos traseiros, incluindo os impactos de um porto recentemente construído e da subida do nível do mar. A evolução da linha de costa foi medida com o sistema de análise digital da linha de costa para períodos de ~10 anos antes e depois da construção do porto. Depois, foi realizada uma análise de inundações utilizando uma nova metodologia baseada em SIG para medir a extensão da inundação utilizando o nível total da água (marés + tempestade + subida do nível do mar) e uma extensão de inundação associada. Finalmente, as tendências de recuo pós-histórico foram incorporadas na análise de inundação para determinar a influência do porto na extensão da inundação. Os resultados mostram que as alterações da linha de costa relacionadas com a construção do porto estão concentradas em torno do porto, enquanto que o resto da área de estudo tende para a estabilidade. A nova metodologia de determinação da extensão de inundação mostra que a aldeia está razoavelmente protegida para os cenários actuais e 2050 dos níveis totais de água com um período de retorno de 1 ano, mas seria afectada por períodos de retorno de 100 anos, especialmente em 2050. O recuo da linha de costa na área mostra impactos mínimos na extensão da inundação em comparação com a subida do nível do mar. Para evitar inundações nos próximos 30 anos, medidas simples como a elevação das dunas, a realimentação sedimentar em locais-chave, e a protecção da vegetação dos sapais podem ser muito eficazes. Para 2100, ambos os cenários (períodos de retorno de 1 ano e 100 anos) mostram uma aldeia altamente impactada que exigirá medidas de adaptação relevantes para que mantenha a sua habitabilidade após 2050, uma vez que todas as principais infra-estruturas seriam inundadas numa base anual.

Palavras-chave: riscos costeiros, inundação, gestão costeira, subida do nível do mar, evolução da linha de costa

Acknowledgments

I would first like to thank my directors. Óscar thank you for your patience, thorough comments, and wise suggestions, it shows that you care a lot about what you do and are excellent at it, and for this reason it has been a pleasure working with you. André, thank you for involving me and trusting me for a project that you care so much about (Culatra 2030 – Sustainable Energy Community), I hope my small contribution can help the community in the long run.

Then, I would like to thank my partner Jonathan for your infinite patience, your suggestions, and for supporting me along the way. To my good friends Azzurra and Giovanni, thank you for the moral support and for your input, it definitely made the whole thing seem much more doable. I would also like to thank my family and friends that supported me from across the Atlantic, I love you all.

To Lara, thank you so much for your help with the shoreline extraction and analysis, your time and patience were much appreciated.

Finally, I have to thank the projection authors for developing and making the sea-level rise projections available, multiple funding agencies for supporting the development of the projections, and the NASA Sea-Level Change Team for developing and hosting the IPCC AR6 Sea-Level Projection Tool.

Table of Contents

List of Figures

List of Tables

List of Abbreviations

CICeoE: Centro de Informação Geospacial do Exército

DEM: Digital Elevation Model

DGT: Direção Geral do Território

DSAS: Digital Shoreline Analysis System

GMSL: Global Mean Sea Level

IPCC: International Panel on Climate Change

MSL: Mean Sea Level

NaN: Not a Number

NSM: Net Shoreline Movement

RMSE: Root Mean Square Error

SLR: Sea level rise

SSP: Shared Socio-economic Pathways

TWL: Total Water Level

WLR: Weighted Linear Regression

1. Introduction

Global mean temperatures have been unceasingly warming for every decade since 1850 inducing fast climate change (IPCC, 2021). One of the main consequences of climate change is sea level rise (SLR) caused mostly by increasing ocean temperatures (inducing thermal expansion) and the melting of ice caps. From 2006 to 2018, the global mean sea level (GMSL) has increased at rates between 3.2 and 4.7 mm/yr, which represents a faster rate than any observed in the past three millennia (IPCC, 2021).

In the last few decades, coastal sectors around the globe have been increasingly occupied and have undergone many morphological, socio-economic, and environmental changes (Neumann *et al.*, 2015). It is estimated that one billion people currently live in coastal areas below 10 m above high tide level, of which 230 million live below 1 m above high tide level (Kulp & Strauss, 2019). Those coastal communities and environments are therefore extremely vulnerable to coastal hazards like storms and flooding, especially in a fast-changing climate (Neumann *et al.*, 2015). This is especially true in low-lying coastal landforms such as barrier islands (Nave & Rebêlo, 2021; Nienhuis & Lorenzo-Trueba, 2019). Different studies have shown that low-lying coastal areas like coastal wetlands, lagoons, and estuaries are particularly vulnerable to SLR due to their low elevation and their ecological and socio-economic importance (Al-Nasrawi *et al.*, 2021; Blankespoor *et al.*, 2014; Davies-Vollum & West, 2015; Silveira *et al.*, 2021).

The most common way to measure the possible impacts of SLR on the world's coasts is by simply computing a still water level above a digital elevation model (e.g., 1 m higher than current shoreline) (Ferreira *et al.*, 2021). This method is called a "bathtub approach" (Poulter & Halpin, 2008). Yet, this approach maximizes inundation (Lopes *et al.*, 2022; Poulter & Halpin, 2008; Williams & Lück-Vogel, 2020), especially with SLR lower than 1 m (Li *et al.*, 2014), because it does not include the future land elevation variation, which can be induced by marsh growth or coastal erosion (Poulter & Halpin, 2008), does not consider the infiltration of the water in the sand or the surface roughness (Li *et al.*, 2014; Lopes *et al.*, 2022; Poulter & Halpin, 2008; Williams & Lück-Vogel, 2020), and assumes a long-lasting water level (Li *et al.*, 2014). In order to obtain more accurate results, several authors have attempted to develop methodologies to improve the simple bathtub approach due to the overestimation of its results (e.g., Li *et al.*,

2014; Terres de Lima *et al.*, 2021; Williams & Lück-Vogel, 2020). One of the main challenges in modelling coastal inundations include different environmental responses toward coastal flooding (e.g., open ocean coast vs. backbarrier estuary). Therefore, due to the high variability of the global coastal geomorphology, SLR impacts can only be evaluated precisely at local scales (Cazenave & Cozannet, 2014). Moreover, different types of coastal flooding (e.g., storm surge related flood, SLR related inundation, and wave related flood) cannot be modeled equally.

In addition to the flooding hazard, coasts of the world are greatly affected by human influences, such as coastal urbanization (Elliott *et al.*, 2019; Halpern *et al.*, 2007), pollution (Defeo *et al.*, 2009; Halpern *et al.*, 2007), disruption of natural sediment regimes (Carrasco *et al.*, 2012a; Defeo *et al.*, 2009; Hsu *et al.*, 2007; Kombiadou *et al.*, 2019), destruction of coastal environments (e.g. mangroves and marshes) (Elliott *et al.*, 2019; Halpern *et al.*, 2007), and infrastructure construction (El-Asmar *et al.*, 2016; Halpern *et al.*, 2007; Hsu *et al.*, 2007; Kombiadou *et al.*, 2019; Sakhaee & Khalili, 2021). These disruptions of the natural coastal environment have numerous impacts on the coastal environments, especially on sandy ones (Yincan, 2017), and are expected to increase in the future (Neumann *et al.*, 2015; Vousdoukas *et al.*, 2020).

More specifically, the construction of ports and harbors is known to significantly influence the hydrodynamics, sediment regimes, and ecosystems of coastal environments (Barbaro *et al.*, 2019; El-Asmar *et al.*, 2016; Shenghui *et al.*, 2018). The most common morphological impacts induced by the construction of harbors are erosion, scour, and sedimentation (Sakhaee and Khalili, 2021). Various case studies on the topic have been published in the recent years in open ocean and sea environments (e.g. Barbaro *et al.*, 2019; Duarte *et al.*, 2018; Ghaderi *et al.*, 2020; Sakhaee & Khalili, 2021; Shenghui *et al.*, 2018; Song *et al.*, 2017), estuaries (e.g. El-Asmar *et al.*, 2016; Prumm and Iglesias, 2016), and lakes (e.g. Mattheus and Diggins, 2019), but very few have discussed the morphological impacts of harbor construction in backbarrier environments.

Understanding how the increase in TWL combined with anthropized shorelines will impact coastal occupation is necessary to maintain the safety of the communities and infrastructures. To do so, this study intends to compare the shoreline evolution of a small village in the South

of Portugal (Culatra) before and after the construction of a harbor and beach nourishment, and to include the post-construction trends of shoreline evolution within a coastal flooding analysis. In this same location, Carrasco *et al.* (2013) used a simple bathtub approach to map the potential inundation extension related to SLR in the village of Culatra. Yet, this approach is not ideal in sandy substrates like barrier islands since it does not consider the permeability of the soil that can strongly limit flooding. In addition, that study did not integrate and compare the potential impact of the shoreline evolution in the flooding simulations.

The specific objectives of this study will be to:

1. Define the morphological evolution of Culatra's backbarrier shoreline before and after the construction of the harbor and the coastal nourishment.
2. Assess the vulnerability of the village to inundation by extreme total water levels based on scenarios of SLR and shoreline retreat.
3. Propose coastal management measures based on the observed coastline's evolution and the potential flooding due to TWL.

2. Study Area

2.1. Location and Context

The study area is the village of Culatra, and surrounding coastline located on the center of the backbarrier of Culatra Island, one of the five islands of the Ria Formosa barrier system in the South of Portugal (Fig. 1). The Ria Formosa natural park includes the biggest coastal lagoon environment in Portugal with an area of 84 km^2 (Andrade, 1990). It extends for approximately 55 km in the W-E direction and between ~ 0.5 and 8 km in the N-S direction. It is protected by five barrier islands – Barreta, Culatra, Armona, Tavira, and Cabanas – and two peninsulas – Ancão and Cacela (Fig. 1). The topography of the islands is dominated by vegetated dunes with a continuous frontal dune of c. 5 to 10 m high on the oceanside (Pilkey *et al.*, 1989). The lagoon side was formed by the accumulation of fine sands and its colonization by halophile vegetation creating large sand tidal flats and salt marshes (Pilkey *et al.*, 1989). Today, these tidal flats and salt marshes represent two thirds of the whole lagoon area (Carrasco *et al.*, 2021) and the lagoon has an average depth of less than 2 m below mean sea level (MSL) (Andrade, 1990).

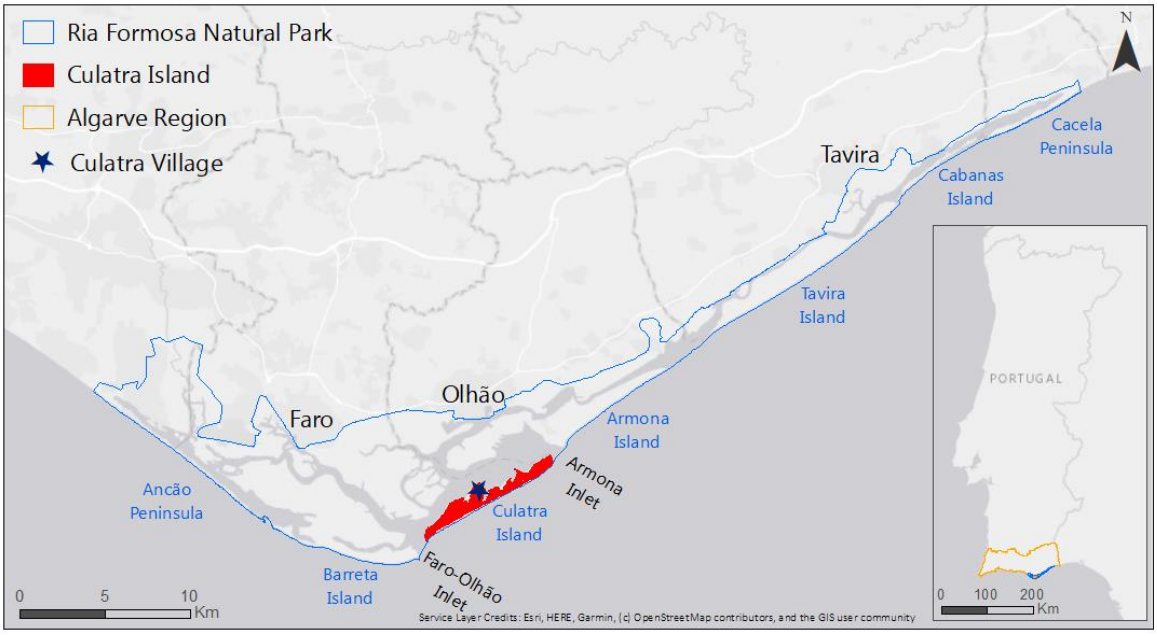

Figure 1. Location of Culatra Island and village within the Ria Formosa in southern Portugal.

Culatra Island is located in the center West of the Ria Formosa between Faro-Olhão Inlet on the West and Armona Inlet on the East. The island is approximately 7.45 km long. The eastern part of the island has an average width of ~479 m while it is ~387 m in the western side (Garcia

et al., 2010). The island comprises three villages: Farol, Hangares, and Culatra (Fig. 2A). Culatra village is the largest and the only one with permanent occupation (Hidroprojecto, 2005) (Fig. 2B, 2C). The whole island has a permanent population of ~1000 people, although it triples during the summer (May to September) due to tourism (Pacheco *et al.*, 2021). The two main economic activities are related to fishing and mollusc farming, and tourism (Pacheco *et al.*, 2021). The vast majority of the buildings on the island are residential homes, with some commercial and municipal infrastructures (Carrasco *et al.*, 2013). Many of those infrastructures are located less than 100 m from the sea, putting them potentially at risk of inundation (Carrasco *et al.*, 2013). Between 2007 and 2011, a fishers' harbor was built in Culatra village (Fig. 2C), which interfered with the evolution of the coastline in the area.

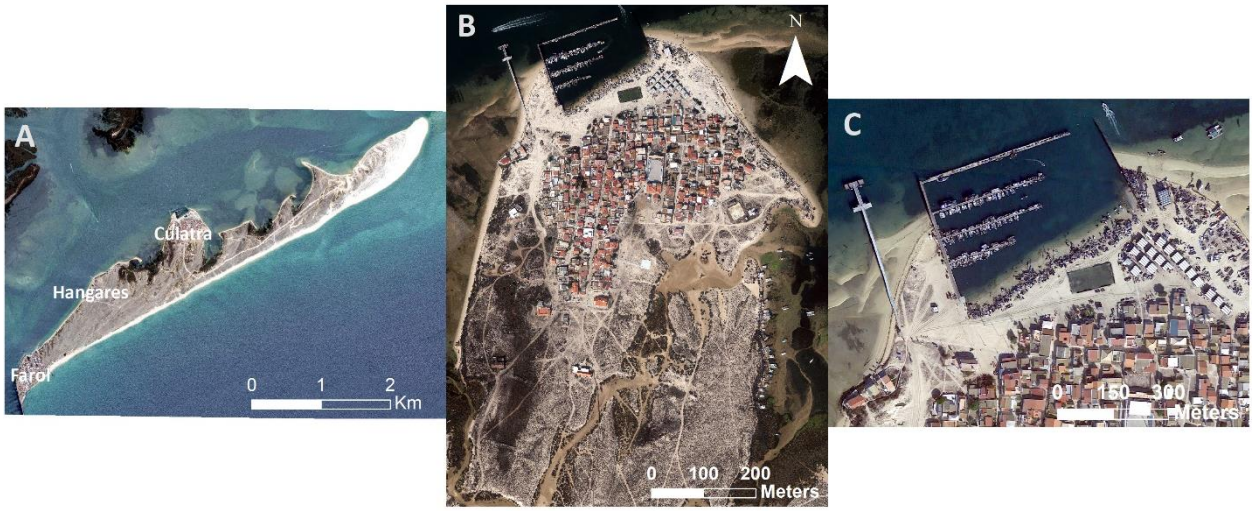

Figure 2. A) Culatra Island and its three villages: Farol, Hangares, and Culatra. B) Culatra village. C) Detailed view of the recently built harbor in Culatra village and the nourishment that took place in the vicinity of the harbor to avoid the periodical inundation of the buildings. Images from Google Earth.

2.2. Hydrodynamic of the Area

Due to its position relatively far from the inlets and on the backbarrier, Culatra village is rather sheltered from the most energetic ocean related storm impacts. Since the fetch is very limited (maximum ~6 km in Culatra) in the lagoon, it doesn't allow the formation of high and long waves (Carrasco *et al.*, 2011).

Tides are the major sediment transport mechanism within the Ria Formosa (Salles *et al.*, 2005), the tidal regime is semidiurnal mesotidal. The typical average tidal ranges are 2.8 m for spring tides, with a maximum range of 3.5 m, and 1.3 m for neap tides (Carrasco *et al.*, 2009; Ferreira *et al.*, 2016; Pacheco *et al.*, 2008, 2011).

Based on surge values during 11 storms from 1990 to 2009, the average storm surge height was 0.36 m at the Huelva Tide Gauge in Spain, located ~80 km from the Ria Formosa, with a maximum recorded height of 0.42 m (Almeida *et al.*, 2012).

Localized projections of SLR have been developed by Fox-Kemper *et al.* (2021) and Garner *et al.* (2021-a-b) based on the different shared socio-economic pathways (SSP) presented in the latest report from the international panel on climate change (IPCC, 2021). For the Algarve, the closest projections available are in Lagos, approximately 80 km to the East of the study area (Table 1). The median *likely* confidence level rates of SLR are predicted to be 6.8 mm/yr (SSP 3-7.0), 7.3 mm/yr (SSP 5-8.5), and 7.8 mm/yr (low confidence SSP 5-8.5) between 2040 and 2060 and 10.1 mm/yr (SSP 3-7.0), 12.1 mm/yr (SSP 5-8.5), and 16.0 mm/yr (low confidence SSP 5-8.5) between 2080 and 2100 (Fox-Kemper *et al.*, 2021; Garner *et al.*, 2021-a-b).

Table 1. Sea Level Rise (SLR) projections from 2030 to 2150 in Lagos, Portugal according to five different Shared Socio-economic Pathways (SSP) scenarios. The SLR values are present in a *likely* confidence level: the first value represents the median between the 17th and the 83rd percentile (showed in parenthesis). Data and information adapted from IPCC (2021); Fox-Kemper *et al.* (2021); Garner *et al.*, (2021-a-b).

	Sea level rise according to five SSP (m)					
Year	SSP 1-1.9	SSP 1-2.6	SSP 2-4.5	SSP 3-7.0	SSP 5-8.5	SSP 5-8.5 (low confidence)
2030	0.12 (0.05, 0.19)	0.11 (0.07, 0.17)	0.12 (0.07, 0.16)	0.11 (0.07, 0.16)	0.12 (0.08, 0.16)	0.12 (0.08, 0.17)
2050	0.21 (0.12, 0.32)	0.22 (0.14, 0.31)	0.23 (0.16, 0.32)	0.24 (0.17, 0.33)	0.26 (0.18, 0.35)	0.26 (0.18, 0.40)
2090	0.39 (0.26, 0.57)	0.42 (0.29, 0.61)	0.51 (0.37, 0.72)	0.59 (0.44, 0.80)	0.66 (0.51, 0.90)	0.73 (0.51, 1.20)
2100	0.43 (0.28, 0.63)	0.47 (0.32, 0.68)	0.59 (0.42, 0.83)	0.70 (0.53, 0.96)	0.80 (0.61, 1.08)	0.91 (0.61, 1.45)
2150	0.64 (0.38, 0.98)	0.69 (0.41, 1.07)	0.95 (0.61, 1.41)	1.19 (0.84, 1.69)	1.33 (0.92, 1.95)	2.02 (0.92, 5.18)

2.3. Morphological Evolution of Culatra Island

The morphology of Culatra Island, its coastline, and backbarrier shoreline have been highly altered by the opening and stabilization of the Faro-Olhão Inlet between 1929 and 1955, and the different engineering works that took place until 1955, and in the 1980's (Pacheco *et al.*, 2011). Before these anthropogenic alterations of the system, the dominant inlet of the Ria Formosa was Armona Inlet, but between 1873 and 2009, it has narrowed at a rate of about 30 m/yr (Pacheco *et al.*, 2011). The human interventions in the Faro-Olhão Inlet completely modified the tidal prism of this inlet and adjacent ones, which disrupted the morphology of Culatra Island. The most notable morphological change is the elongation of the island to the

East by ~3000 m between c. 1950 and 2015 (Garcia *et al.*, 2010; Kombiadou *et al.*, 2018, 2019; Nave and Rebêlo, 2021).

The opening and stabilization of the Faro-Olhão Inl*et al*so impacted the backbarrier of Culatra Island by reducing the flow through Armona Inlet which forced Armona's ebb-delta shoals to migrate inshore with the increased actions of the waves and flood tidal currents (Pacheco *et al.*, 2011). This resulted in the overall eastern extension of Culatra's backbarrier by 38% when comparing the area from 1952 with the one from 2014 (Kombiadou *et al.*, 2019).

In addition to the eastern extension of Culatra's backbarrier, Carrasco *et al.* (2008) identified a strong landward migration (coastal squeeze) and coastline increase in both cross- and long-shore backbarrier of Culatra Island between 1947 and 2001. This overall tendency is most likely related to the increased long-shore size of the island itself, combined with the decreased sediment flushing capacity from Armona Inlet (Kombiadou *et al.*, 2018). Localized erosive areas might be related to anthropogenic pressures such as navigation and shellfish harvesting, for instance (Kombiadou *et al.*, 2018).

More locally, the construction of the fishers' harbor and the beach nourishments in its vicinity between 2007 and 2011 is another factor affecting the morphology of Culatra village. The harbor was built to provide a space for fishers to park their boats in safe conditions, sheltered from the waves and with boarding and disembarking gangways to avoid accidents (Hidroprojecto, 2005). Another aim of the project was to protect the cultural and natural heritage of the Ria Formosa since the ~100 boats were previously anchored in front of the village damaging the lagoon bed and its ecosystem (Hidroprojecto, 2005). In the past, several flooding events caused damages to residences and other infrastructures (Carrasco *et al.*, 2013). Preventing the consequences of such events was therefore another motivation for the construction of the harbor and the nourishments of the surrounding beaches.

The harbor construction began in 2007 and was finalized in 2011. The construction consists of two small jetties on the eastern and western sides joined in the North by a floating breakwater (Fig. 2C). It has a parking capacity of 150 boats. To increase the safety of boat traveling from and to the harbor, a canal of 1.5 m below the MSL was dredged, which represented a total of 49 500 m^3 of sand (Hidroprojecto, 2005). On land, the interventions consisted in elevating the

shores on both sides of the harbor to 4.5 m higher than MSL and regulating the beach with a slope inclination of 1:4. Further beach nourishments have taken place between 2014 and 2015 on the west side of the harbor, but the exact amount of sand nourished is unknown (A. Pacheco, personal communication).

3. Methodology

3.1. Shoreline Evolution

The backbarrier shorelines were extracted from a set of eight images covering the 1996-2021 period (26 years). The set included two historical aerial photos (1996 and 1999) and two orthophotographs (2002 and 2014) that were provided by the Centro de Informação Geospacial do Exército (CICeoE) and the Direção Geral do Território (DGT). To increase the temporal resolution of the analyzed period, Google Earth images were used to complete the time period up to 2021. The Google Earth images were downloaded in maximum quality (pixel density of 4800 x 3047) for the years 2007, 2011, 2017, and 2021. The downloading process was done at an eye altitude of 613 m while ensuring no image tilting. Three images per year covering the study area were downloaded in order to increase the image quality, one for the northern part of the village (e.g., 2007_1), one for the southern part of the village (e.g., 2007_2), and one for the coastline adjacent to the village on the East (e.g., 2007_3) (Table 2). To facilitate the georeferencing of the aerial images and orthophoto, they were separated in two sections, one for the West and another one for the East side of the study area. An already available georeferenced orthophoto from 2014 projected in ETRS 1989 Portugal TM06 was used as the base image for the georeferencing of the rest of the images due to its high resolution (pixel size of 0.01 m). All the images were georeferenced using four to six reference points (depending on the size of the image and its quality) with the georeferencing tool from ArcMap 10.8 (ESRI, 2019).

To ensure the accuracy of the georeferencing process, the root mean square error (RMSE) was calculated for each image. Ten control points were drawn sparsely across each image in different locations than the points used for the georeferencing. Then, the coordinates from the predicted (georeferenced image) and correct (referenced 2014 orthophoto) control points were extracted in order to calculate the RMSE. The residuals squared for each point were calculated by subtracting the predicted coordinates from the correct ones in X and Y and squaring the results. The RMSE in X and Y was calculated using equation 1:

$$RMSE\ in\ X\ or\ Y = \frac{\sqrt{\sum(squared\ residuals\ in\ X\ or\ Y)}}{number\ of\ control\ points} \quad (1)$$

The total RMSE was then calculated using equation 2:

$$Total\ RMSE = \sqrt{(X\ residuals)^2 + (Y\ residuals)^2} \quad (2)$$

The total RMSE precision for the Google Earth images and aerial photos (Table 2) were deemed acceptable when lower than 0.4 m.

Table 2. X, Y, and Total root mean square error (RMSE) for each georeferenced image. For the Google Earth images, 2007_1 corresponds to the northwest image from 2007, 2007_2 corresponds to the southwest image from 2007, and 2007_3 corresponds to the eastern image, for instance. As for the aerial photos and orthophotos, the 1996_W corresponds to the village area, while the 1996_E corresponds to the coastline adjacent to the east of the village, for instance.

	Image	X RMSE (m)	Y RMSE (m)	Total RMSE (m)
Google Earth images	2007_1	0.105	0.025	0.108
	2007_2	0.303	0.185	0.355
	2007_3	0.106	0.017	0.108
	2011_1	0.268	0.105	0.287
	2011_2	0.251	0.086	0.266
	2011_3	0.288	0.118	0.311
	2017_1	0.142	0.033	0.146
	2017_2	0.152	0.038	0.157
	2017_3	0.279	0.172	0.328
	2021_1	0.263	0.103	0.283
	2021_2	0.100	0.012	0.101
	2021_3	0.137	0.022	0.139
Aerial photos and orthophoto	1996_W	0.325	0.150	0.357
	1996_E	0.327	0.215	0.392
	1999_W	0.275	0.125	0.302
	1999_E	0.173	0.050	0.180
	2002_W	0.212	0.068	0.223
	2002_E	0.128	0.021	0.129

For most of the areas, except in the vicinity of the harbor and the coast on the East of the harbor, the edge of the stable vegetation (the transition line between the beach sand and the bushy and rugose vegetation) was chosen as the proxy for the backbarrier shoreline (Fig. 3A), as was done by Kombiadou *et al.* (2019). In the absence of such vegetation (e.g., due to coastal occupation), the dune scarp was used as the shoreline proxy, when present (Fig. 3B). Finally, where none of the previous features were present, the highest water level was used, identified by the inward line formed by the accumulation of zoostera or debris (Fig. 3C). The shorelines were also divided into two different groups, the regular shorelines, and the artificially stabilized shorelines, for instance on the harbor jetties. The artificially stabilized shorelines were excluded from the calculations of the shoreline evolution.

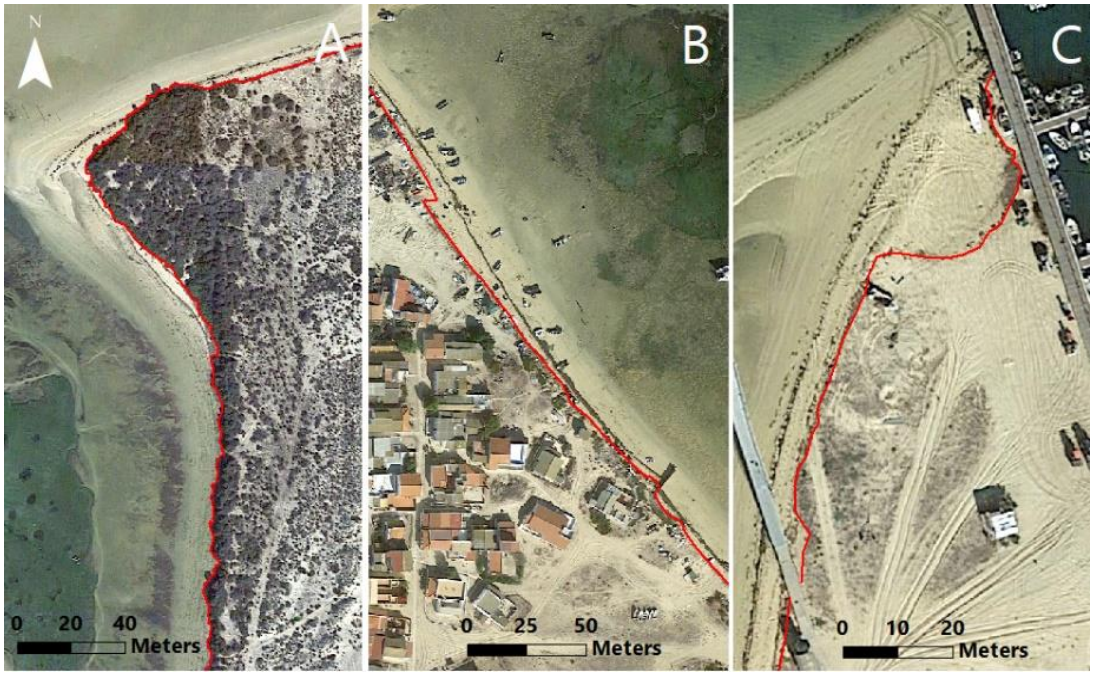

Figure 3. Examples of the features used to map the regular shorelines. A) Use of stable vegetation. B) Dune scarp, when no stable vegetation was present. C) Maximum high-water level when no stable vegetation or dune scarp were present.

To understand the morphological impacts of the harbor on the area, the digital shoreline analysis system (DSAS) version 5.1 (Himmelstoss *et al.*, 2018) was used to compute the shoreline evolution before (1996 to 2007) and after (2011 to 2021) the harbor's implementation and the beach nourishment. First, a baseline was drawn offshore from the different shorelines before and after the harbor construction. Then, transects were placed every 15 m perpendicular to the baseline while covering all the shorelines. The uncertainty used for the DSAS computations are the ones from the georeferencing (Table 2). The uncertainty related to the shoreline mapping was minimized since the shorelines were mostly extracted at the same zoom level and by the same operator.

Five shoreline evolution measurements were calculated with a confidence interval of 95%: the shoreline change envelope (SCE), net shoreline movement (NSM), end-point rate (EPR), linear regression rate (LRR), and weighted linear regression (WLR). In this study, the WLR was used as it is the most statistically robust since it puts more emphasis on the data with lower uncertainties (Himmelstoss *et al.*, 2018).

The shoreline displacement was considered stable when within the georeferencing and mapping error, a small erosion/accretion between the error and two times the error, and strong erosion/accretion when above three times the error (Table 3). The observed trends on

the pre-harbor results were grouped into thirteen sectors according to their similarity to facilitate the analysis (e.g., similar erosive transects in the same area were grouped in a zone). The same sectors were also used to analyze the post-harbor trends.

Table 3. Classification of the trends obtained with the weighted linear regression (WLR) rates and the color code associated with each class.

Classification	WLR (m/yr)	Color Code
Strong Retreat	≤ -0.8	
Small Retreat	]-0.8; -0.4[	
Stable	[-0.4; 0.4]	
Small Accretion	]0.4; 0.8[	
Strong Accretion	≥ 0.8	

3.2. Flooding Cartography

To determine the inundation hazard, a new flood mapping methodology was elaborated based on the definition of the total flood extension and presents an alternative to the widely used simple bathtub approach. A LiDAR digital elevation model (DEM) was used as the elevation proxy of the area. It was obtained from the Direção-Geral do Território (DGT) and has a precision of 2 m horizontally and < 30 cm vertically (Sistema Nacional de Informação Geográfica, 2011). The relevant files representing the study area were merged and projected in ETRS 1989 Portugal TM06.

The total water level (TWL = tides + surge + SLR) was used to compute and map the potentially flooded areas according to different SLR scenarios. The predicted SLR values used were based on the latest IPCC report for Lagos, Portugal (Fox-Kemper *et al.*, 2021; Garner *et al.*, 2021-a-b) (Table 1). The average SSP 5-8.5 was used since it is the scenario that will be observed at a global scale if the greenhouse gas emissions are not drastically reduced in the coming decades (IPCC, 2021), and is the most widely used for future climate change impact simulations. The storm surge and maximum tide levels were adapted from Carrasco *et al.* (2012a) (Table 4).

Table 4. Total water levels used in this study based on the tides and storm surge levels computed by Carrasco *et al* (2012a). The return periods are for the tides + surge levels. The total water levels are presented for the current scenario and the median *likely* SSP 5-8.5 scenario from the IPCC report from 2021 (Fox-Kemper *et al.*, 2021; Garner *et al.*, 2021-a-b) in Lagos, Portugal for two years of reference: 2050, and 2100.

Return Period (years)	Total Water Level (m)		
	Current	2050	2100
1	2.02	2.28	2.82
100	2.48	2.74	3.28

First, the simple bathtub approach (Poulter & Halpin, 2008) of each flooding scenario was applied on the DEM to determine the potentially flooded areas. The pixels with higher altitudes than the ones for each level were reclassified as "not a number" (NaN), i.e., they would not be flooded even when using the simple bathtub approach. Based on the reclassified values for each scenario, a cost distance analysis was performed in ArcMap as the first step to define the flood extension. The dune crest (higher elevation near the beach/dune contact) was used as the origin for the distance computation (flooding source). The water depth (h_c) was calculated with the Raster Calculator by subtracting the elevation of each pixel from the flood level for each scenario. The Raster Calculator was also used to compute the flooding velocity (u_c) according to the expression developed by Donnelly (2008) for overwash in sandy beaches:

$$u_c = 1.53\sqrt{g h_c} \quad (3)$$

where g is the acceleration of gravity. u_c was considered as a proxy for the flood velocity on the absence of an equation specifically developed for tide + surge + SLR.

Finally, the Raster Calculator was used to apply the expression from Plomaritis *et al.* (2018) that defines the potential flooding extension:

$$h(x) = h_c \exp\left(-a \frac{x}{u_c}\right) \quad (4)$$

where h(x) represents the water elevation at a distance x from the flooding source, h_c is the water depth, a is a constant associated to the rate of infiltration of the water in the soil. In this study, the constant 0.12 was used as the infiltration value because it is a typical one for barrier islands like Culatra (Donnelly *et al.*, 2006 in Plomaritis *et al.*, 2018). x represents the distance from the flooding source, and u_c is the overwash/flooding velocity.

In addition to the six scenarios described in Table 4, two others were added with the TWL of 2050 for 1-year and 100-year return periods but this time including a projection of the shoreline retreat for 2050. The average shoreline evolution trends of the five sectors surrounding the village were computed to determine which were retreating. To do so, the trend of each transect contained in each zone was averaged to determine a general trend for the zone. The erosive zonal trends were included in a second flooding simulation for 2050. A new position of the dune crest was estimated for 2050 by multiplying by 29 years ((2050-

2021) +1) the average zonal trend, e.g., the average shoreline retreat for zone 5 was -0.72 m/yr, the dune crest was therefore displaced inland by 20.98 m for the second simulation. This new dune crest was used as the origin for the cost distance analysis (x value) and the overwash/flooding extension.

After computing the overwash/flooding extension, the values with an inundation value < 1 cm were considered meaningless and were removed for the final cartography. In addition, the non-hydraulically connected polygons were removed from the cartography i.e., areas that are considered flooded by the cartography but are not connected to a flooding source (Poulter & Halpin, 2008). The "four-side rule" was used in this study, meaning that only the cells related to a flooded one through one of the four sides of the pixel were considered hydraulically connected (Poulter & Halpin, 2008).

Finally, the flooded areas for each scenario were compared to the occupied areas of the village. A shapefile was created with the different occupied areas (buildings, main walking paths, football field, helipad, etc.) and was intersected with the flooded sectors to determine the part of the occupied areas that would be flooded according to the TWL scenarios.

4. Results

4.1. Shoreline Evolution

The shoreline evolution for about 10 years before (1996-2007), and after (2011-2021) the harbor construction was measured with the DSAS. The WLR results for the whole studied area reveal only a few statistically significant transects (between 3.98% and 8.72%) under a confidence interval of 95%. This means that according to the WLR analysis performed, between ~4% and ~9% of the transects had significant erosion or accumulation either before or after the harbor construction. Nonetheless, trends can be analyzed due to high coherence in the results. The comparisons between the different statistical analysis show strong relationships, especially before the harbor construction (Annex I). The post-harbor trends are also very similar for all performed statistics, mainly after removing the two outliers with the highest uncertainty (Annex I). This supports the reliability of the used method (WLR).

The results of the cost-distance analysis are presented in Annex II and III.

The shoreline trends before the harbor construction reveal numerous stable areas (sectors 1, 4, 7, 8, and 11) with some accretional (sectors 2, 3, 5, 9, and 13) and erosional (sectors 10, and 12) hotspots (Fig. 4A). It also had more active tidal channels in zone 1 (breaks in the shoreline continuity) compared to after the harbor construction. The shoreline trends after the harbor construction show more extensive erosional (sectors 2, 3, 5, and 6) and accretional (zone 4) sectors around the village, but greater stability on the eastern shoreline, outside the village (sectors 8 to 13) (Fig. 4B). The harbor area and its vicinity, sectors 2, 3, and 5 show a clear shift in behavior: they were accretional pre-harbor and shifted to erosional after the harbor construction. Conversely, zone 4 evolved from stable to highly accretional. (Fig. 4A, B).

Of the 172 pre-harbor transects evaluated, 74 were erosional (43.02%), and 98 were accretional (56.98%), while after the harbor construction, 87 transects were erosional (49.43%), and 89 were accretional (50.57%) for a total of 176 transects analyzed.

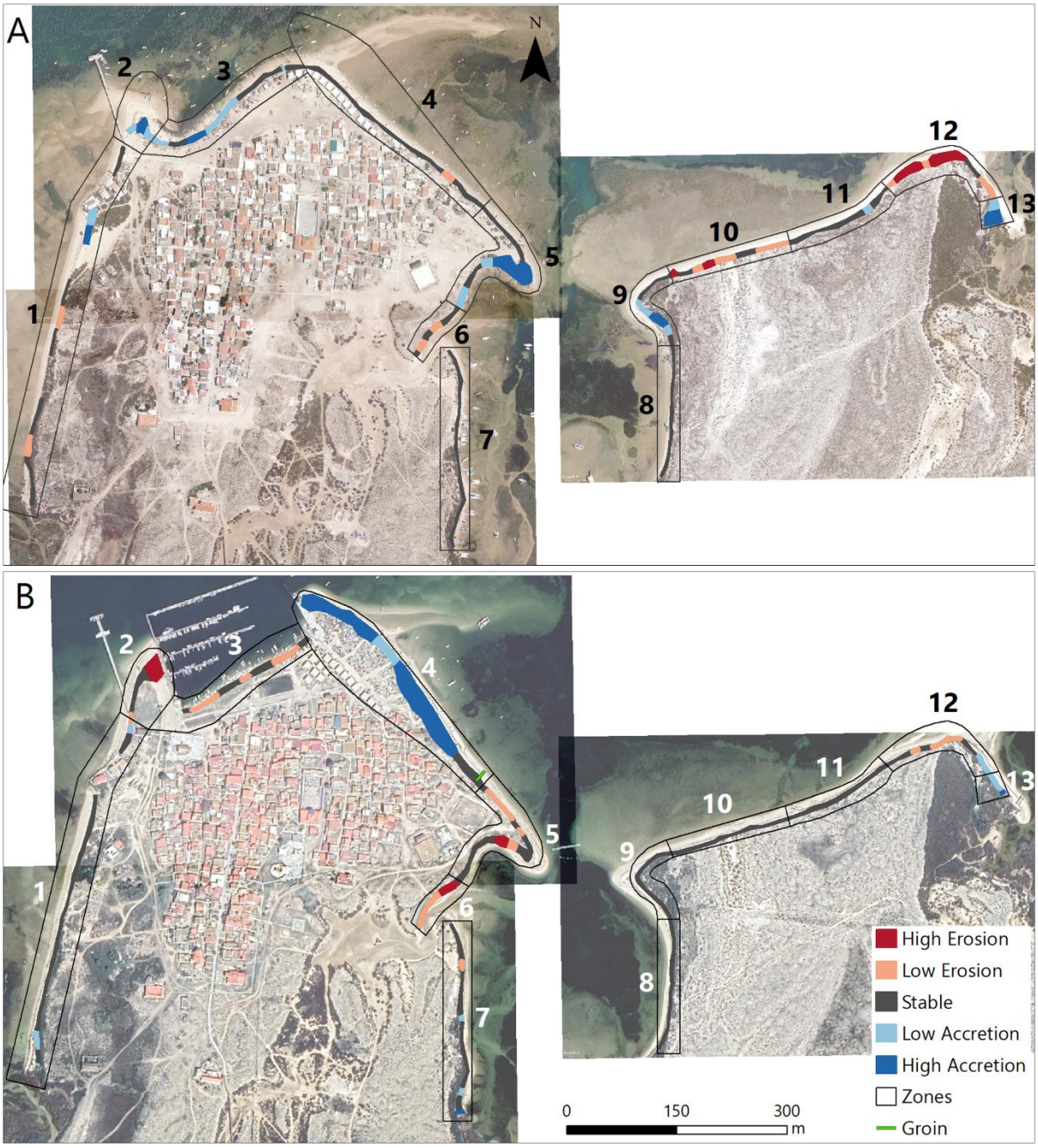

Figure 4. Weighted Linear Regression Rates (m/yr) (A) before (1996-2007) and (B) after (2011-2021) the harbor construction and the beach nourishment. The similar pre-harbor trends were divided into sectors (polygons 1 to 13) to facilitate the analysis. The color display on the mapping was determine according to the accepted error (Table 3).

The convention for the shoreline trends is that positive values represent accreting shorelines while negative values represent eroding ones. The global average WLR rates were 0.1 m/yr before and after the harbor construction. The maximum WLR erosion rates were -1.3 m/yr before the harbor construction (Fig. 4A, 5A – Zone 12), and -1.6 m/yr after (Fig. 4B, 5B – Zone 2). On the other end, the maximum pre-harbor accretional rate was 2.6 m/yr (Fig. 4A, 5A – Zone 5), while the post-harbor one was 2.3 m/yr (Fig. 4B, 5B – Zone 4).

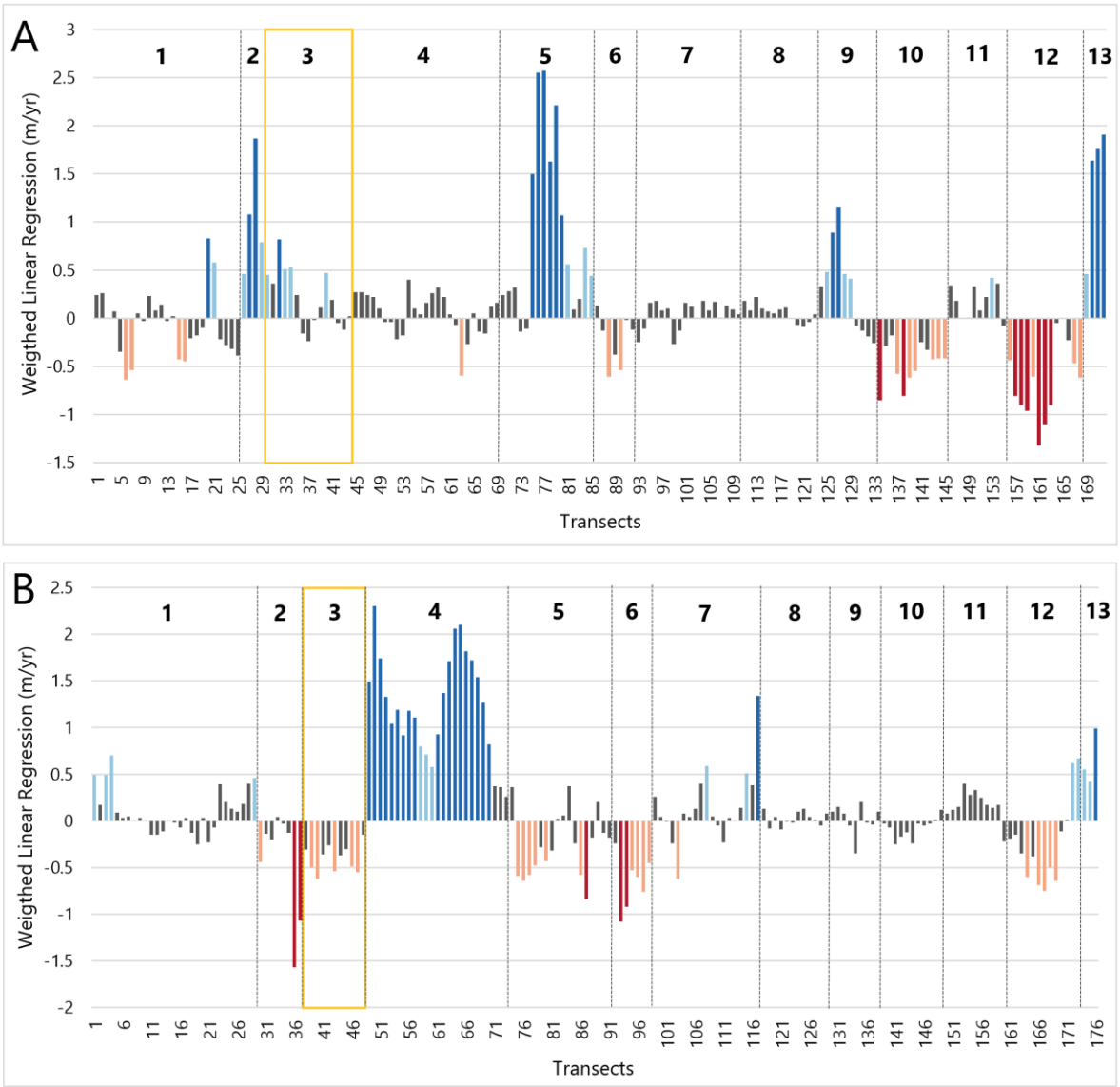

Figure 5. Weighted linear regression rates (m/yr) for each transect analyzed (A) before and (B) after the harbor construction and the beach nourishment. The numbers above each section of the graphs represent the different sectors from figure 4. The yellow rectangles represent the harbor area.

4.3. Flooding Cartography

The flooding impacts are minimal for the current scenario with a 1-year return period and even considering the 100-year return period, but extensive for the 2100 scenario namely when considering the 100-year return period (Fig. 6). The flooding shows a high horizontal expansion between 2050 and 2100 (Fig. 6). The flooding extension for 2050 with a return period of 100 years is very similar to the one for 2100 with a 1-year return period, indicating that what is presented as an extreme event in ~30 years could be very common in ~80 years.

For each scenario, the flooding is further inland on the West side of the harbor compared to the East one (Fig. 6). The flooding through the tidal channel in the South is minimal in all scenarios except for the 2100 ones (Fig. 6).

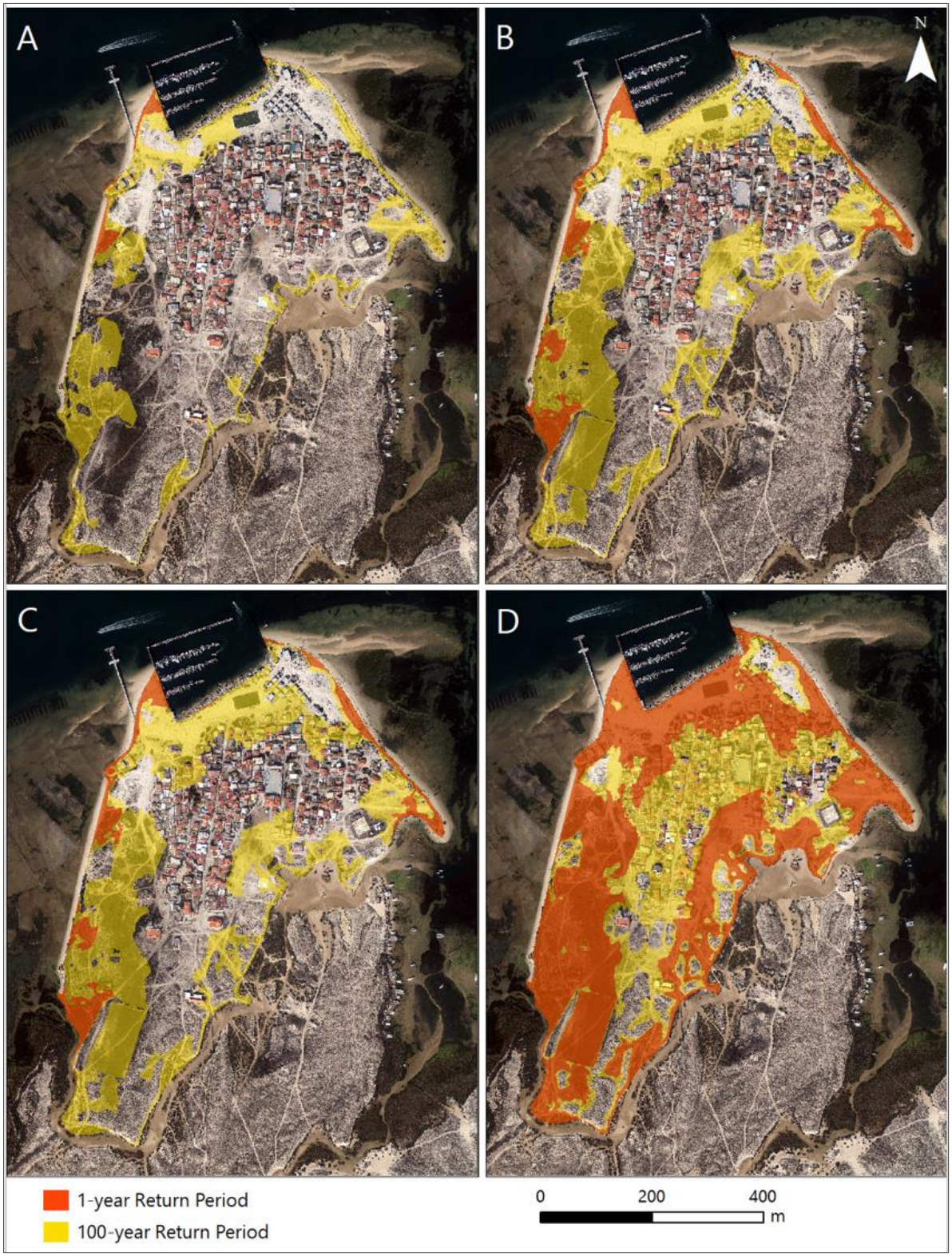

Figure 6. Flooding cartography results for return periods of 1 year (orange) and 100 years (yellow). A) Current scenario. B) 2050 scenario. C) 2050 scenario including the average shoreline retreat rates projected in 2050 for sectors 2, 3, 5, and 6 (Fig. 5B). D) 2100 scenario.

The four erosive average trends found in the sectors around the village were projected for the year 2050. Those sectors are 2, 3, 5, and 6 (Fig. 4B) with respective average rates of -0.44 m/yr, -0.40 m/yr, -0.25 m/yr, and -0.72 m/yr. In 2050, this would represent an average shoreline retreat of -12.8 m (Zone 2), -11.7 m (Zone 3), -7.2 m (Zone 5), and -21.0 m (Zone 6) (Fig. 7).

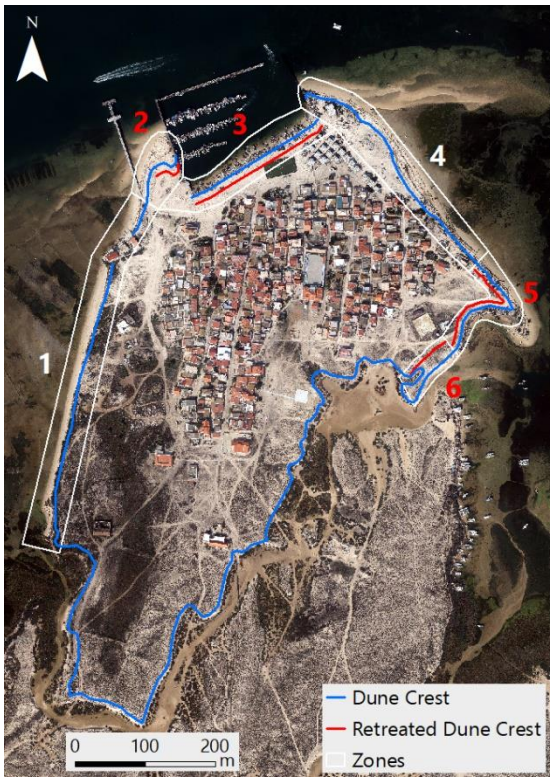

Figure 7. Dune crests used as the proxies for the cost distance analysis. The blue line represents the current dune crest while the red ones represent the future dune crest based on the average shoreline retreat of the eroding sectors from the shoreline analysis (Fig. 4).

The shoreline retreat has minimal flooding impact compared to the increase in TWL due to SLR (Table 5). The 1-year return period flooding extension in 2050 with and without shoreline retreat would be identical (Table 5), although the 100-year return period results reveal a more extensive inundated area within the harbor (zone 3) and the eastern spit (sectors 5 and 6) (Fig. 4; Fig. 6). Considering the shoreline retreat in the analysis would cause the flooding of 3136 m^2 on the eastern part of zone 3, and in zone 5 compared to the results without including it (Table 5).

When comparing the return periods, a 100-year return period would increase the flooded area by 19.32% in the present scenario, 40.35% in 2050, 40.87% in 2050 when including the shoreline retreat, and 32.43% in 2100, compared to the 1-year return period of the same year (Table 5).

Table 5. Flooded areas according to the different scenarios of total water level used in this study, the occupied areas related that would be flooded, and the proportion they represent compared to the whole occupied area.

Scenario	Flooded Area (m^2)	Flooded Occupied Area (m^2)	Flooded Occupied Area (%)
Current 1-yr RP	2 837	153	0.13
Current 100-yr RP	59 761	5 488	4.60
2050 1-yr RP	17 841	1 454	1.22
2050 100-yr RP	136 741	27 545	23.11
2050 1-yr RP (Retreat)	17 841	1 454	1.22
2050 100-yr RP (Retreat)	139 876	30 365	25.47
2100 1-yr RP	158 689	39 437	33.08
2100 100-yr RP	254 160	102 216	85.75
Total	294 632	119 202	

The present scenario with a 1-year return period occasions minimal impact to the occupied area since it would only flood some walking paths. In 2050 with a 100-year return period, with or without shoreline retreat, the flood would reach the main village and not only affect isolated houses and the football field, but also restaurants, the helipad, the community center, fishing huts, and main walking paths (Fig. 6). The potential flooding in 2100 with a 100-year return period would impact almost 86% of the occupied area (Table 5), which includes all the main infrastructures of the village.

5. Discussion

5.1. Influence of the Harbor Construction on the Shoreline Evolution

The evolution of a backbarrier shoreline is usually very slow (Carrasco *et al.*, 2011), and due to the small timescale studied (~10 years before and after the harbor construction), the evolution trend results were often within the error, and had to be considered stable. The number of years analyzed could also explain the low significance of the results (all transects had a significance level below 10% under a confidence level of 95%). Nonetheless, the results obtained within this study were highly coherent, and values above the obtained error can be considered as representative of the observed evolution. Overall, the results show a coastline evolving very slowly, but that undeniably changed since the harbor construction and associated beach nourishment, especially in the vicinity of said harbor.

The main difference in zone 1 before (Fig. 4A, 5A) and after the harbor construction (Fig. 4B, 5B) is the strong decrease in the number of active tidal channels. These tidal channels have been artificially blocked by the community of the village to avoid the flooding of this area (O. Ferreira, personal communication).

The accretion observed before the harbor construction in zone 2 (Fig. 4A, 5A) was most likely caused by the accumulation of sediments transported by the dominant currents within this area of the Ria Formosa (Pacheco *et al.*, 2008). These sediments accumulated as recurved small spits and eventually, around 2007, attached to the main shoreline. This zone in the vicinity of the harbor was completely modify with the construction works since it was subject to nourishment which altered its natural evolution. The strong erosion observed after the harbor construction and nourishment could be related to the readjustment of the slope and of the overall morphology to a more natural one for this area. Human activities such as boat launching and tractors movement to transport materials and merchandises are also very important, which could promote the erosion and the lowering of the area, allowing an inland displacement of the water line. In addition, this zone is also affected by wakes generated by ferry boats and the boats passages from and toward the harbor. These wakes can promote the resuspension of sediments which can alter the topo-bathymetry of the backbarrier shoreline (Herbert *et al.*, 2018).

The small erosive trend within the harbor (Fig. 4B, 5B – Zone 3) could again be related to strong human activities and a readjustment of the slope following the harbor construction and the nourishment. Sectors 4 and 5 were previously stable and in accretion, but the combination of the construction of the harbor and the groin disturbed their evolution. The shoreline trends of sectors 4, 5, and 6 (Fig. 4B, 5B) are intrinsically related due to the construction of a small groin between sectors 4 and 5 (Fig. 4B). A strong accumulation then arose in zone 4 while sectors 5 and 6 were sediment deprived, indicating a dominant northwest-southwest longshore transport in the coastal sector. The construction of the groin appears to have had a greater influence on the evolution of zone 4 than the harbor one. The beach nourishment in the vicinity of the harbor could have encouraged the sediment accumulation on the North of the groin. Finally, the erosion and accumulation seen in sectors 12 and 13 before the harbor construction decreased afterwards, indicating that this section of the shoreline is almost stable and doesn't show any impact from the harbor construction.

Carrasco *et al.* (2008) observed a landward displacement of Culatra Island between 1947 and 2001, and its backbarrier was classified as immature in 2001. In comparison, according to Kombiadou *et al.* (2019), the western part of Culatra's backbarrier (including Culatra village) was relatively stable between 1952 and 2014 and the salt marshes were classified as stable to immature during the same time period. It is therefore possible to assume that the harbor construction and associated beach nourishment could have interfered with the maturing process that the backbarrier and salt marshes were going through. A longer interval can be expected before reaching complete marshes and backbarrier stability, especially considering the future uncertainties related to climate change.

5.2. Potential Flooding in Culatra Village

The inundation results showed that for a 1-year return period for current and 2050 scenarios, the occupied flooded areas would be minimal. However, the village would be greatly impacted by an inundation occasioned by a 100-year return period. This indicates that the village is somewhat protected for the near future recurrent TWL, but will need some adaptations to prepare against future major TWL since the flooded occupied areas increase drastically for the 2050 scenario with a 100-year return period and between 2050 and 2100 (Table 5).

The obtained results are in accordance with the field observations during the Emma Storm in 2018 (TWL return period of 6-7 years) (Ferreira *et al.*, 2019), when no flooding was observed within the main village. They seem to disagree with Lopes *et al.* (2022) which state that the backbarrier of Culatra would be almost completely flooded between 2046 and 2065 with a 2-year return period. They also disagree with the results from Carrasco *et al.* (2013), and Antunes (2019) and Antunes *et al.* (2019) that have been made publicly available by the Portuguese government (see https://arcg.is/0u5XnL) which suggest that Culatra Island would be strongly flooded by 2050. These last works consider the areas as impermeable and the TWL as a permanent inundation level that affects the entire area regardless of their position or hydraulic connectivity in the case of Antunes (2019) and Antunes *et al.* (2019). Thus, they maximize the flooded area to a level that is not consistent with reality. This study provides a more precise flood mapping of Culatra village compared to the studies mentioned above since the developed methodology consider water infiltration and dune crest retreat. This is relevant since presenting exaggerated results to the public can have counterproductive effects by discrediting the relevance of climate change science (Lopes *et al.,* 2022).

The scenarios used in this study and the ones from the studies presented above did not include a morphodynamic feedback induced by flood events, i.e., a readjustment of the dune crest or the dune area due to higher water levels. The increased flooding frequency and intensity would promote dune lowering and eventually dune loss, which represents a positive morphodynamic feedback that can lead to more flooding events. This kind of feedback could be especially problematic in locations where sedimentation rates are lower than SLR, which would occasion strong coastal retreats (Zhou *et al.*, 2022). The assessment of such feedbacks would require more complex modelling, hence their exclusion from this study.

One of the most important factors when modelling the potential inundation hazard is the TWL used. Despite the fact that the SLR projections developed by IPCC (2021) are the most accurate and recent ones in the literature at the moment, they still contain uncertainties – mostly related to the future greenhouse gas emissions – that could considerably change the SLR projections. The median value for the high confidence scenario (SSP 5-8.5) was considered representative of future condition but a wide range of scenarios could be tested with different results. The projections of TWL used in this study also assume that the past storm surge and tidal levels will remain the same over the next century. However, Vousdoukas *et al.* (2016) showed that

storm surge levels along the southern Portuguese coast could slightly decrease within this century, which would also slightly decrease the TWL and therefore the extension of inundations. Pickering *et al.* (2017) studied the impacts of SLR on tidal levels and showed that when increasing the global water level by 2 m, the mean high-water level could increase by 0.05 m when considering coastal retreat or on the opposite decrease by 0.02 m when considering a fixed present-day coastline. A further increase in water level could facilitate the propagation of long waves (e.g., tidal waves) inside the lagoon by reducing bottom friction, which in turn would increase the inundation levels, the opposite is also true (Lopes *et al.*, 2022). This could particularly be an important factor for the West side of the village, which is the most impacted among the scenarios, but is also the area where the vegetation is highest and most stable. The presence of stable vegetation on this side of the village could increase bottom friction and decrease the flooding velocity and extension. On the contrary, the presence of several impermeable concrete walking paths within the island would prevent the infiltration of the water and facilitate the propagation of the tidal wave further inland. The expansion of the flood would increase the risk to the occupied area including places with higher social and economical value (e.g., community center, restaurants, and helipad). These paths are nevertheless small and in limited amounts within the study area.

Another important factor for inundation mapping is the quality of the elevation model used (Poulter & Halpin, 2008). In this case, the DEM used is relatively old (2011) considering that the shoreline has evolved since, and that other beach nourishments and terrain modifications have taken place in the last 11 years. The model also contained some errors regarding the elimination of the elevated features such as buildings (some areas showed elevations above 4 m shaped as a perfect squares). It was however considered to be representative of the vast majority of the area in its present condition since the dune morphology is stable and only a relatively small portion of the area was anthropically altered.

The main limitation of the new methodology developed in this study is that the formula used was developed for overwash i.e., temporary floods caused by waves, while it was used here to determine a higher duration inundation (during high tide) and thus the obtained velocities are most likely exaggerated. However, the time over which the flood occurs allows a continuity of the flow and probably counterbalances that exaggeration. Apart from that limitation, this new methodology includes several advantages that makes it a good option to map inundations in

sandy backbarrier coasts. Firstly, the slope is considered in the computations of the water propagation inland, as it was computed in other methodologies (e.g., Didier *et al.*, 2019; Perini *et al.*, 2016; Sekovski *et al.*, 2015; Terres de Lima *et al.*, 2021; Williams & Lück-Vogel, 2020), since the elevation relatively to the water level is computed for each pixel. Secondly, the use of the cost distance analysis (also used by Li *et al.*, 2014; Perini *et al.*, 2016; Sekovski *et al.*, 2015; Williams & Lück-Vogel, 2020) allows a more accurate assessment of the possibility of the propagation of the water inland compared to the simple bathtub approach. One of the improvements regarding the cost distance tool used in this study is that the analysis was repeated to determine the potential flooding impacts related to coastal erosion to provide a more complete estimation of the flooding potential of the area, including the potential shoreline evolution by 2050. The additional analysis provided more information on the importance of shoreline retreat in the coastal flooding of Culatra village and proved that the inundation mostly depends on SLR and TWL increases rather than coastal erosion. The main improvement of this methodology compared to most of the ones presented above is that it includes the infiltration of the water in the soil which can be an important decreasing water level factor in sandy substrate like barrier islands.

5.3. Coastal Management Measures to Mitigate the Impacts of Coastal Flooding and Erosion

At the moment, Culatra village is one of the only two communities within the Ria Formosa who do not suffer from erosion due to its location on the backbarrier, protected from open ocean related hazards (Ceia *et al.*, 2010). But the TWL inundation related to SLR hazard is substantial.

In the last few decades, the use of soft stabilization (e.g., beach nourishment, vegetation, restauration of wetlands, dune creation, etc.) has become a more popular approach compared to the use of hard stabilization (e.g., groin, jetty, breakwater, revetment, etc.) (Bilkovic *et al.*, 2016; Ceia *et al.*, 2010; Sharma *et al.*, 2016; Waltham *et al.*, 2021). The "soft-engineering" measures typically have lower environmental impacts which makes them better candidates for fragile systems like the Ria Formosa (Ceia *et al.*, 2010).

Different measures can be considered to allow the community to remain in Culatra village. For the current scenario and the 2050 one with a 1-year return period, no protection measures are

necessary since the occupied flooded areas are mostly walking paths that will need to be cleaned after the storm or extreme water level.

For the current and 2050 scenarios with return periods of 100 years, several measures should be considered to protect the community. On the West of the harbor (Fig. 4, zone 2) where erosion has been the highest of the study area since the harbor construction, transport with tractors should be limited, if not forbidden and displaced where the concrete ramp is on the East side within the harbor. This reduction of anthropic disturbances should be coupled with the restauration of native plants. According to Feagin *et al.* (2009), coastal vegetation is a great way to modify and control the sedimentary dynamics of an area in response to slow events like tidal forces or SLR. Further nourishing the area without a reduction of the human disruptions preventing the development of stable vegetation would lead to the same result in ten years without solving the problem in the long-term. If reducing the use of this location is not an option, then the implementation of a new ramp should be considered. The ramp should be at least as high as the highest adjacent dune crest to prevent flooding through it. Similarly, human actions on the shoreline within the harbor should be avoided to protect it and allow vegetation to grow and create a buffer between the waterline and the village. The use of the ramp on the East side within the harbor should be enforced to promote the long-term safety of the inhabitants. In the tidal channel on the South of the village, the vegetation is already well implemented and not too disturbed, therefore elevating the dunes could be a good option to further protect this area from flooding. This method could prevent the inundation of several features such as the helipad, a playground, a kindergarten, and houses. Finally, with the rates of accretion observed in zone 4 (Fig. 4; Fig. 5), it is safe to assume that the flooded area in zone 4 in 2050 would most likely be attenuated since the shoreline has moved between 10 and 25 m forward since the DEM data was acquired in 2011. Therefore, no particular intervention is recommended for this area.

For the 2100 scenarios, the viability of the village itself is threaten by floods that would affect all the main infrastructures and many houses on a yearly basis. If the scenarios for 2100 presented in this study actually came to reality, simple measures like the ones mentioned above (e.g., dune elevation, nourishment, and marsh vegetation) would mostly likely not be enough to protect the village and its inhabitants. Thus, three main solutions can be considered. The first option would be to use hard protection all around the village, for instance by building

concrete walls or dikes, though this solution would highly decrease the quality of life of the habitants and would be very expensive. In addition to the hard protection, some parts of the village might need to be rebuilt on an elevated and stabilized ground, which would further increase the price of this option.

The second and safest option for the community would be to relocate. Though, studies have shown that many people living in coastal communities will remain in place and accept to live at risk because they are emotionally attached to the location, the environment, or their community, or for the proximity with their workplace and/or public facilities (Buchori *et al.*, 2018; Costas *et al.*, 2015). Furthermore, a study about the perception of risk in a coastal community within the Ria Formosa, Praia de Faro, showed that householders (both fishers and touristic communities) are convinced that the ocean related hazards threatening their barrier island is not something that will affect them within their lifetime, even if coastal managers know that it will have severe consequences for those people (Costas *et al.*, 2015). Since the fishing community from Praia de Faro is comparable to the one in Culatra village, it is possible to assume that the risk perception is similar within the two communities.

That said, if the community wants to remain in this flood prone area until the end of the century, many changes will be needed. The third option is therefore adaptation. First, a sensibilization program should be implemented to present the hydro-meteorological hazards and their potential consequences for the population. This program should include different options for the population, including timeframes. For individual house owners, apart from relocation, long-term solutions could be to elevate the houses above a potential water level or to use an amphibious architecture (see English *et al.*, 2016), solutions that are already used in many locations worldwide (Buchori *et al.*, 2018; English *et al.*, 2016; Liao *et al.*, 2016; Proverbs & Lamond, 2017). Typically, building a flood resistant or amphibious house will increase the costs by 5 to 10% compared to a normal house. Unless the authorities decide to invest in that kind of architecture, the financial costs would be assumed by individuals. Knowing the risks of living in a flood prone area, public authorities should ensure that all new constructions are water resistant or resilient to guaranty the safety of the people and attenuate future economic, social, and health disasters. Other less expensive solutions for homeowners already established in the village could be to redesign their house according to potential floods, for instance by adding high storage space, raising electrical sockets and panels, moving furniture ahead of a

storm, etc. (Proverbs & Lamond, 2017). But in order for the community to remain safe and prepare their houses for storm related floods, an early warning system and an evacuation plan should be put in place by the authorities and practiced with the community as soon as possible.

6. Conclusions

The goals of this study were to evaluate the impacts that the construction of the harbor and beach nourishment had on the shoreline evolution of the area, to determine future shoreline position in order to include it in the TWL flooding scenarios, and to evaluate the vulnerability of the village and propose management measures to attenuate the risks. The shoreline positions were extracted from aerial photographs, orthophotos, and Google Earth images for periods of 11 years before the harbor construction and 10 years after. A new methodology was developed to assess the potential inundation extension and different TWL for current, 2050, and 2100 scenarios with storm surge and high tide levels with return period of 1 year and 100 years.

Culatra's shoreline has seen mild changes outside the harbor and its vicinity since the harbor completion in 2011. The sectors inside the harbor and directly to the West of it have seen major erosion trends in the last 11 years compared to the rest of the area. These trends could be attributed to a combination of wakes, human activities, and slope readjustment. On the opposite, the East side of the harbor has seen strong accretion since 2011 that could be attributed to the construction of a groin downstream which also caused the downdrift sectors to be sediment deprived. As for the flooding vulnerability, the new methodology shows that the village would not see any major floods from the current and 2050 scenarios with a 1-year return periods but would be affected by a 100-year return period. Both scenarios from 2100 show high vulnerability of the village that would require major changes in planning and architecture in order for the community to remain safe. The variation of TWL appears to have a greater influence on the inundation extension compared to shoreline retreat for this area.

For the next 30 years, relatively easy measures can be taken to avoid important flood related damages like elevating dunes and nourishing more flood prone areas. However, considering the continuity of the island occupation after 2050, more thorough analysis must be undertaken to provide the community with practical and realistic solutions.

References

Almeida, L. P., Vousdoukas, M. V., Ferreira, Ó., Rodrigues, B. A., & Matias, A. (2012). Thresholds for Storm Impacts on an Exposed Sandy Coastal Area in Southern Portugal. *Geomorphology*, *143–144*, 3–12. https://doi.org/10.1016/j.geomorph.2011.04.047

Al-Nasrawi, A. K. M., Kadhim, A. A., Shortridge, A. M., & Jones, B. G. (2021). Accounting for DEM Error in Sea Level Rise Assessment within Riverine Regions; Case Study from the Shatt Al-Arab River Region. *Environments*, *8*(5), 46. https://doi.org/10.3390/environments8050046

Andrade, C. A. (1990). *O Ambiante de Barreira da Ria Formosa, Algarve, Portugal* [Ph.D Thesis]. Universidade de Lisboa.

Antunes, C. (2019). Assessment of Sea Level Rise at West Coast of Portugal Mainland and Its Projection for the 21st Century. *Journal of Marine Science and Engineering*, *7*(3), 61. https://doi.org/10.3390/jmse7030061

Antunes, C., Rocha, C., & Catita, C. (2019). Coastal Flood Assessment due to Sea Level Rise and Extreme Storm Events: A Case Study of the Atlantic Coast of Portugal's Mainland. *Geosciences*, *9*(5), 239. https://doi.org/10.3390/geosciences9050239

Barbaro, G., Foti, G., Miduri, M., & Puntorieri, P. (2019). Shoreline Changes Caused by Marina of Badolato (Italy). *International Journal of Civil Engineering and Technology*, *10*(7), 298–307.

Bilkovic, D. M., Mitchell, M., Mason, P., & Duhring, K. (2016). The Role of Living Shorelines as Estuarine Habitat Conservation Strategies. *Coastal Management*, *44*(3), 161–174. https://doi.org/10.1080/08920753.2016.1160201

Blankespoor, B., Dasgupta, S., & Laplante, B. (2014). Sea-Level Rise and Coastal Wetlands. *AMBIO*, *43*(8), 996–1005. https://doi.org/10.1007/s13280-014-0500-4

Buchori, I., Pramitasari, A., Sugiri, A., Maryono, M., Basuki, Y., & Sejati, A. W. (2018). Adaptation to coastal flooding and inundation: Mitigations and migration pattern in Semarang City, Indonesia. *Ocean & Coastal Management*, *163*, 445–455. https://doi.org/10.1016/j.ocecoaman.2018.07.017

Carrasco, A. R., Ferreira, Ó., Davidson, M., Matias, A., & Dias, J. A. (2008). An Evolutionary Categorisation Model for Backbarrier Environments. *Marine Geology*, *251*(3–4), 156–166. https://doi.org/10.1016/j.margeo.2008.02.009

Carrasco, A. R., Ferreira, Ó., Freire, P., & Dias, J. A. (2009). Morphological Changes in a Low-Energy Backbarrier. *Journal of Coastal Research*, *1,* 173–177.

Carrasco, A. R., Ferreira, Ó., & Matias, A. (2013). Managing Flood Risk in Fetch-Limited Environments. *Journal of Coastal Research*, *65*, 892–897. https://doi.org/10.2112/SI65-151.1

Carrasco, A. R., Ferreira, Ó., Matias, A., & Freire, P. (2012a). Natural and Human-induced Coastal Dynamics at a Back-Barrier Beach. *Geomorphology*, *159–160*, 30–36. https://doi.org/10.1016/j.geomorph.2012.03.001

Carrasco, A. R., Ferreira, Ó., Matias, A., & Freire, P. (2012b). Flood Hazard Assessment and Management of Fetch-Limited Coastal Environments. *Ocean & Coastal Management*, *65*, 15–25. https://doi.org/10.1016/j.ocecoaman.2012.04.016

Carrasco, A. R., Ferreira, Ó., Matias, A., Pacheco, A., & Freire, P. (2011). Short-Term Sediment Transport at a Backbarrier Beach. *Journal of Coastal Research*, *277*, 1076–1084. https://doi.org/10.2112/JCOASTRES-D-09-00163.1

Cazenave, A., & Cozannet, G. L. (2014). Sea level rise and its coastal impacts. *Earth's Future*, *2*(2), 15–34. https://doi.org/10.1002/2013EF000188

Ceia, F. R., Patrício, J., Marques, J. C., & Dias, J. A. (2010). Coastal Vulnerability in Barrier Islands: The High Risk Areas of the Ria Formosa (Portugal) System. *Ocean & Coastal Management*, *53*(8), 478–486. https://doi.org/10.1016/j.ocecoaman.2010.06.004

Costas, S., Ferreira, O., & Martinez, G. (2015). Why do we decide to live with risk at the coast? *Ocean & Coastal Management*, *118*, 1–11. https://doi.org/10.1016/j.ocecoaman.2015.05.015

Davies-Vollum, K. S., & West, M. (2015). Shoreline Change and Sea Level Rise at the Muni-Pomadze Coastal Wetland (Ramsar site), Ghana. *Journal of Coastal Conservation*, *19*(4), 515–525. https://doi.org/10.1007/s11852-015-0403-y

Defeo, O., McLachlan, A., Schoeman, D. S., Schlacher, T. A., Dugan, J., Jones, A., Lastra, M., & Scapini, F. (2009). Threats to Sandy Beach Ecosystems: A Review. *Estuarine, Coastal and Shelf Science*, *81*(1), 1–12. https://doi.org/10.1016/j.ecss.2008.09.022

Didier, D., Baudry, J., Bernatchez, P., Dumont, D., Sadegh, M., Bismuth, E., Bandet, M., Dugas, S., & Sévigny, C. (2019). Multihazard Simulation for Coastal Flood Mapping: Bathtub Versus Numerical Modelling in an Open Estuary, Eastern Canada. *Journal of Flood Risk Management*, *12*(S1). https://doi.org/10.1111/jfr3.12505

Donnelly, C. (2008). *Coastal Overwash: Processes and Modelling* [Ph.D Thesis]. Lund University.

Duarte, C. R., de Miranda, F. P., Landau, L., Souto, M. V. S., Sabadia, J. A. B., Neto, C. Â. da S., Rodrigues, L. I. de C., & Damasceno, A. M. (2018). Short-Time Analysis of Shoreline Based on RapidEye Satellite Images in the Terminal Area of Pecém Port, Ceará, Brazil. *International Journal of Remote Sensing*, *39*(13), 4376–4389. https://doi.org/10.1080/01431161.2018.1457229

El-Asmar, H. M., Taha, M. M. N., & El-Sorogy, A. S. (2016). Morphodynamic Changes as an Impact of Human Intervention at the Ras El-Bar-Damietta Harbor coast, NW Damietta Promontory, Nile Delta, Egypt. *Journal of African Earth Sciences*, *124*, 323–339. https://doi.org/10.1016/j.jafrearsci.2016.09.035

Elliott, M., Day, J. W., Ramachandran, R., & Wolanski, E. (2019). A Synthesis: What Is the Future for Coasts, Estuaries, Deltas and Other Transitional Habitats in 2050 and Beyond? In *Coasts and Estuaries* (pp. 1–28). Elsevier. https://doi.org/10.1016/B978-0-12-814003-1.00001-0

English, E., Klink, N., & Turner, S. (2016). Thriving with water: Developments in amphibious architecture in North America. *E3S Web of Conferences*, *7*, 13009. https://doi.org/10.1051/e3sconf/20160713009

ESRI. (2019). *ArcGIS Desktop* (10.8.0.12790) [Computer software]. ESRI inc.

Feagin, R. A., Lozada-Bernard, S. M., Ravens, T. M., Möller, I., Yeager, K. M., & Baird, A. H. (2009). Does Vegetation Prevent Wave Erosion of Salt Marsh Edges? *Proceedings of the National Academy of Sciences*, *106*(25), 10109–10113. https://doi.org/10.1073/pnas.0901297106

Ferreira, Ó., Kupfer, S., & Costas, S. (2021). Implications of Sea-Level Rise for Overwash Enhancement at South Portugal. *Natural Hazards*, *109*(3), 2221–2239. https://doi.org/10.1007/s11069-021-04917-0

Ferreira, Ó., Matias, A., & Pacheco, A. (2016). The East Coast of Algarve: A Barrier Island Dominated Coast. *Thalassas: An International Journal of Marine Sciences*, *32*(2), 75–85. https://doi.org/10.1007/s41208-016-0010-1

Ferreira, Ó., Plomaritis, T. A., & Costas, S. (2019). Effectiveness Assessment of Risk Reduction Measures at Coastal Areas Using a Decision Support System: Findings from Emma Storm. *Science of The Total Environment*, *657*, 124–135. https://doi.org/10.1016/j.scitotenv.2018.11.478

Fox-Kemper, B., H. T. Hewitt, C. Xiao, G. Aðalgeirsdóttir, S. S. Drijfhout, T. L. Edwards, N. R. Golledge, M. Hemer, R. E. Kopp, G. Krinner, A. Mix, D. Notz, S. Nowicki, I. S. Nurhati, L. Ruiz, J-B. Sallée,

A. B. A. Slangen, Y. Yu. (2021). Ocean, cryosphere and sea level change. In: Climate Change 2021: The Physical Science Basis. Contribution of Working Group I to the Sixth Assessment Report of the Intergovernmental Panel on Climate Change [Masson-Delmotte, V., P. Zhai, A. Pirani, S. L. Connors, C. Péan, S. Berger, N. Caud, Y. Chen, L. Goldfarb, M. I. Gomis, M. Huang, K. Leitzell, E. Lonnoy, J. B. R. Matthews, T. K. Maycock, T. Waterfield, O. Yelekçi, R. Yu and B. Zhou (eds.)]. Cambridge University Press. In press.

Garcia, T., Ferreira, Ó., Matias, A., & Dias, J. A. (2010). Overwash Vulnerability Assessment Based on Long-term Washover Evolution. *Natural Hazards*, *54*(2), 225–244. https://doi.org/10.1007/s11069-009-9463-3

Garner, G. G., T. Hermans, R. E. Kopp, A. B. A. Slangen, T. L. Edwards, A. Levermann, S. Nowikci, M. D. Palmer, C. Smith, B. Fox-Kemper, H. T. Hewitt, C. Xiao, G. Aðalgeirsdóttir, S. S. Drijfhout, T. L. Edwards, N. R. Golledge, M. Hemer, R. E. Kopp, G. Krinner, A. Mix, D. Notz, S. Nowicki, I. S. Nurhati, L. Ruiz, J-B. Sallée, Y. Yu, L. Hua, T. Palmer, B. Pearson (2021a). IPCC AR6 sea-level rise projections. Version 20210809. PO.DAAC, CA, USA. Dataset accessed [2021-12-03] at https://podaac.jpl.nasa.gov/announcements/2021-08-09-Sea-level-projections-from-the-IPCC-6th-Assessment-Report.

Garner, G. G., R. E. Kopp, T. Hermans, A. B. A. Slangen, G. Koubbe, M. Turilli, S. Jha, T. L. Edwards, A. Levermann, S. Nowikci, M. D. Palmer, C. Smith, in prep. (2021b). Framework for assessing changes to sea-level (FACTS). Geoscientific Model Development.

Ghaderi, D., & Rahbani, M. (2020). Detecting Shoreline Change Employing Remote Sensing Images (Case Study: Beris Port - East of Chabahar, Iran). *International Journal of Coastal and Offshore Engineering*, *3*(4), 1–8. https://doi.org/10.29252/ijcoe.3.4.1

Halpern, B. S., Selkoe, K. A., Micheli, F., & Kappel, C. V. (2007). Evaluating and Ranking the Vulnerability of Global Marine Ecosystems to Anthropogenic Threats. *Conservation Biology*, *21*(5), 1301–1315. https://doi.org/10.1111/j.1523-1739.2007.00752.x

Herbert, D., Astrom, E., Bersoza, A., Batzer, A., McGovern, P., Angelini, C., Wasman, S., Dix, N., & Sheremet, A. (2018). Mitigating Erosional Effects Induced by Boat Wakes with Living Shorelines. *Sustainability*, *10*(2), 436. https://doi.org/10.3390/su10020436

Hidroprojecto. (2005). *Estudo de Impacto Ambiental do Projecto do Porto de Abrigo para a Pequena Pesca na Ilha da Culatra* (Resumo Não Técnico 01.RP-I.004(1); p. 23).

Himmelstoss, E. A., Henderson, R. E., Kratzmann, M. G., & Farris, A. S. (2018). *Digital Shoreline Analysis System (DSAS) version 5.0 user guide: U.S. Geologial Survey Open-File Report 2018-1179* (p. 110). https://doi.org/10.3133/ofr20181179

Hsu, T.-W., Lin, T.-Y., & Tseng, I.-F. (2007). Human Impact on Coastal Erosion in Taiwan. *Journal of Coastal Research*, *234*, 961–973. https://doi.org/10.2112/04-0353R.1

IPCC. (2021). Summary for Policymakers. In *Climate Change 2021: The Physical Science Basis* (Contribution of Working Group I to the Sixth Assessment Report of the Intergovernmental Panel on Climate Change [Masson-Delmotte, V., P. Zhai, A. Pirani, S.L. Connors, C. Péan, S. Berger, N. Caud, Y. Chen, L. Goldfarb, M.I. Gomis, M. Huang, K. Leitzell, E. Lonnoy, J.B.R. Matthews, T.K. Maycock, T. Waterfield, O. Yelekçi, R. Yu, and B. Zhou (eds.)]., p. 40). Intergovernmental Panel on Climate Change.

Kombiadou, K., Matias, A., Carrasco, A. R., Ferreira, Ó., Costas, S., & Vieira, G. (2018). Towards Assessing the Resilience of Complex Coastal Systems: Examples from Ria Formosa (South Portugal). *Journal of Coastal Research*, *85*, 646–650. https://doi.org/10.2112/SI85-130.1

Kombiadou, K., Matias, A., Ferreira, Ó., Carrasco, A. R., Costas, S., & Plomaritis, T. (2019). Impacts of Human Interventions on the Evolution of the Ria Formosa Barrier Island System (S. Portugal). *Geomorphology*, *343*, 129–144. https://doi.org/10.1016/j.geomorph.2019.07.006

Kulp, S. A., & Strauss, B. H. (2019). New elevation data triple estimates of global vulnerability to sea-level rise and coastal flooding. *Nature Communications*, *10*(1), 4844. https://doi.org/10.1038/s41467-019-12808-z

Li, X., Grady, C. J., & Peterson, A. T. (2014). Delineating Sea Level Rise Inundation Using a Graph Traversal Algorithm. *Marine Geodesy*, *37*(2), 267–281. https://doi.org/10.1080/01490419.2014.902884

Liao, K.-H., Le, T. A., & Nguyen, K. V. (2016). Urban design principles for flood resilience: Learning from the ecological wisdom of living with floods in the Vietnamese Mekong Delta. *Landscape and Urban Planning*, *155*, 69–78. https://doi.org/10.1016/j.landurbplan.2016.01.014

Lopes, C. L., Sousa, M. C., Ribeiro, A., Pereira, H., Pinheiro, J. P., Vaz, L., & Dias, J. M. (2022). Evaluation of Future Estuarine Floods in a Sea Level Rise Context. *Scientific Reports*, *12*, 8083. https://doi.org/10.1038/s41598-022-12122-7

Mattheus, C. R., & Diggins, T. P. (2019). Geomorphology of a Harbor-Breakwater Beach along a High Sand-Supply, Wave-Dominated Great Lakes Littoral Cell. *Journal of Coastal Research*, *35*(1), 41. https://doi.org/10.2112/JCOASTRES-D-17-00209.1

Nave, S., & Rebêlo, L. (2021). Coastline Evolution of the Portuguese South Eastern Coast: A High-Resolution Approach in a 65 Years' Time-Window. *Journal of Coastal Conservation*, *25*(1), 7. https://doi.org/10.1007/s11852-020-00791-3

Neumann, B., Vafeidis, A. T., Zimmermann, J., & Nicholls, R. J. (2015). Future Coastal Population Growth and Exposure to Sea-Level Rise and Coastal Flooding—A Global Assessment. *PLOS ONE*, *10*(3), e0118571. https://doi.org/10.1371/journal.pone.0118571

Nienhuis, J. H., & Lorenzo-Trueba, J. (2019). Simulating Barrier Island Response to Sea Level Rise with the Barrier Island and Inlet Environment (BRIE) Model v1.0. *Geophysical Research Letters*, *12*(9), 4013–4030. https://doi.org/10.5194/gmd-12-4013-2019

Pacheco, A., Ferreira, Ó., & Williams, J. J. (2011). Long-Term Morphological Impacts of the Opening of a New Inlet on a Multiple Inlet System. *Earth Surface Processes and Landforms*, *36*(13), 1726–1735. https://doi.org/10.1002/esp.2193

Pacheco, A., Monteiro, J., Santos, J., Sequeira, C., & Nunes, J. (2021). Energy Transition Process and Community Engagement on Geographic Islands: The Case of Culatra Island (Ria Formosa, Portugal). *Renewable Energy*, *184*, 700–711. https://doi.org/10.1016/j.renene.2021.11.115

Pacheco, A., Vila-Concejo, A., Ferreira, Ó., & Dias, J. A. (2008). Assessment of Tidal Inlet Evolution and Stability Using Sediment Budget Computations and Hydraulic Parameter Analysis. *Marine Geology*, *247*(1–2), 104–127. https://doi.org/10.1016/j.margeo.2007.07.003

Perini, L., Calabrese, L., Salerno, G., Ciavola, P., & Armaroli, C. (2016). Evaluation of Coastal Vulnerability to Flooding: Comparison of Two Different Methodologies Adopted by the Emilia-Romagna Region (Italy). *Natural Hazards and Earth System Sciences*, *16*(1), 181–194. https://doi.org/10.5194/nhess-16-181-2016

Pickering, M. D., Horsburgh, K. J., Blundell, J. R., Hirschi, J. J.-M., Nicholls, R. J., Verlaan, M., & Wells, N. C. (2017). The Impact of Future Sea-Level Rise on the Global Tides. *Continental Shelf Research*, *142*, 50–68. https://doi.org/10.1016/j.csr.2017.02.004

Pilkey, O. H., Monteiro, J. H., Dias, J. M. A., & Neal, W. J. (1989). Algarve Barrier Islands: A Noncoastal-Plain System in Portugal. *Journal of Coastal Research*, *5*(2), 239–261.

Plomaritis, T. A., Ferreira, Ó., & Costas, S. (2018). Regional Assessment of Storm Related Overwash and Breaching Hazards on Coastal Barriers. *Coastal Engineering*, *134*, 124–133. https://doi.org/10.1016/j.coastaleng.2017.09.003

Poulter, B., & Halpin, P. N. (2008). Raster Modelling of Coastal Flooding from Sea-level Rise. *International Journal of Geographical Information Science*, *22*(2), 167–182. https://doi.org/10.1080/13658810701371858

Proverbs, D., & Lamond, J. (2017). Flood Resilient Construction and Adaptation of Buildings. In D. Proverbs & J. Lamond, *Oxford Research Encyclopedia of Natural Hazard Science*. Oxford University Press. https://doi.org/10.1093/acrefore/9780199389407.013.111

Prumm, M., & Iglesias, G. (2016). Impacts of port development on estuarine morphodynamics: Ribadeo(Spain). *Ocean & Coastal Management*, *130*, 58–72. http://dx.doi.org/10.1016/j.ocecoaman.2016.05.003

Sakhaee, F., & Khalili, F. (2021). Sediment pattern & rate of bathymetric changes due to construction of breakwater extension at Nowshahr port. *Journal of Ocean Engineering and Science*, *6*(1), 70–84. https://doi.org/10.1016/j.joes.2020.04.002

Salles, P., Voulgaris, G., & Aubrey, D. G. (2005). Contribution of Nonlinear Mechanisms in the Persistence of Multiple Tidal Inlet Systems. *Estuarine, Coastal and Shelf Science*, *65*(3), 475–491. https://doi.org/10.1016/j.ecss.2005.06.018

Sekovski, I., Armaroli, C., Calabrese, L., Mancini, F., Stecchi, F., & Perini, L. (2015). Coupling Scenarios of Urban Growth and Flood Hazards Along the Emilia-Romagna Coast (Italy). *Natural Hazards and Earth System Sciences*, *15*(10), 2331–2346. https://doi.org/10.5194/nhess-15-2331-2015

Sharma, S., Goff, J., Cebrian, J., & Ferraro, C. (2016). A hybrid shoreline stabilization technique: Impact of modified intertidal reefs on marsh expansion and nekton habitat in the northern Gulf of Mexico. *Ecological Engineering*, *90*, 352–360. https://doi.org/10.1016/j.ecoleng.2016.02.003

Shenghui, J., Rijun, H., Xiuli, F., Longhai, Z., Wei, Z., & Aijiang, L. (2018). Influence of the Construction of the Yantai West Port on the Dynamic Sedimentary Environment. *Marine Georesources & Geotechnology*, *36*(1), 43–51. https://doi.org/10.1080/1064119X.2017.1278809

Silveira, F., Lopes, C. L., Pinheiro, J. P., Pereira, H., & Dias, J. M. (2021). Coastal Floods Induced by Mean Sea Level Rise—Ecological and Socioeconomic Impacts on a Mesotidal Lagoon. *Journal of Marine Science and Engineering*, *9*(12), 1430. https://doi.org/10.3390/jmse9121430

Sistema Nacional de Informação Geográfica. (2011). *Modelo Digital do Terreno (Resolução 2 m)—Zonas Costeiras de Portugal Continental—2011*. https://dados.gov.pt/en/datasets/modelo-digital-do-terreno-resolucao-2-m-zonas-costeiras-de-portugal-continental-2011/#_

Song, H., Kuang, C., Liang, H., & Xie, H. (2017). Impacts of Construction of Harbor Projects on Hydrodynamic and Sediment Transport Environments in the Southwest of Bohai Bay. *Journal of Tongji University*, *45*(4), 511–518. http://dx.doi.org/10.11908/j.issn.0253-374x.2017.04.008

Terres de Lima, L., Fernández-Fernández, S., Gonçalves, J. F., Magalhães Filho, L., & Bernardes, C. (2021). Development of Tools for Coastal Management in Google Earth Engine: Uncertainty Bathtub Model and Bruun Rule. *Remote Sensing*, *13*(8), 1424. https://doi.org/10.3390/rs13081424

Vousdoukas, M. I., Ranasinghe, R., Mentaschi, L., Plomaritis, T. A., Athanasiou, P., Luijendijk, A., & Feyen, L. (2020). Sandy Coastlines Under Threat of Erosion. *Nature Climate Change*, *10*(3), 260–263. https://doi.org/10.1038/s41558-020-0697-0

Vousdoukas, M. I., Voukouvalas, E., Annunziato, A., Giardino, A., & Feyen, L. (2016). Projections of Extreme Storm Surge Levels Along Europe. *Climate Dynamics*, *47*(9–10), 3171–3190. https://doi.org/10.1007/s00382-016-3019-5

Waltham, N. J., Alcott, C., Barbeau, M. A., Cebrian, J., Connolly, R. M., Deegan, L. A., Dodds, K., Goodridge Gaines, L. A., Gilby, B. L., Henderson, C. J., McLuckie, C. M., Minello, T. J., Norris, G. S., Ollerhead, J., Pahl, J., Reinhardt, J. F., Rezek, R. J., Simenstad, C. A., Smith, J. A. M., … Weinstein, M. P. (2021). Tidal Marsh Restoration Optimism in a Changing Climate and Urbanizing Seascape. *Estuaries and Coasts*, *44*(6), 1681–1690. https://doi.org/10.1007/s12237-020-00875-1

Williams, L. L., & Lück-Vogel, M. (2020). Comparative Assessment of the GIS Based Bathtub Model and an Enhanced Bathtub Model for Coastal Inundation. *Journal of Coastal Conservation*, *24*(2), 23. https://doi.org/10.1007/s11852-020-00735-x

Yincan, Y. (2017). Coastal Erosion. In *Marine Geo-Hazards in China* (pp. 269–296). Elsevier. https://doi.org/10.1016/B978-0-12-812726-1.00007-3

Zhou, Z., Liang, M., Chen, L., Xu, M., Chen, X., Geng, L., Li, H., Serrano, D., Zhang, H., Gong, Z., & Zhang, C. (2022). Processes, feedbacks, and morphodynamic evolution of tidal flat–marsh systems: Progress and challenges. *Water Science and Engineering*, *15*(2), 89–102. https://doi.org/10.1016/j.wse.2021.07.002

Annex I

Trend comparison for the different statistical analysis performed by the DSAS. The grey colored points (A-B-C) represent the pre-harbor results while the black ones (D-E-F) represent the post-harbor results.

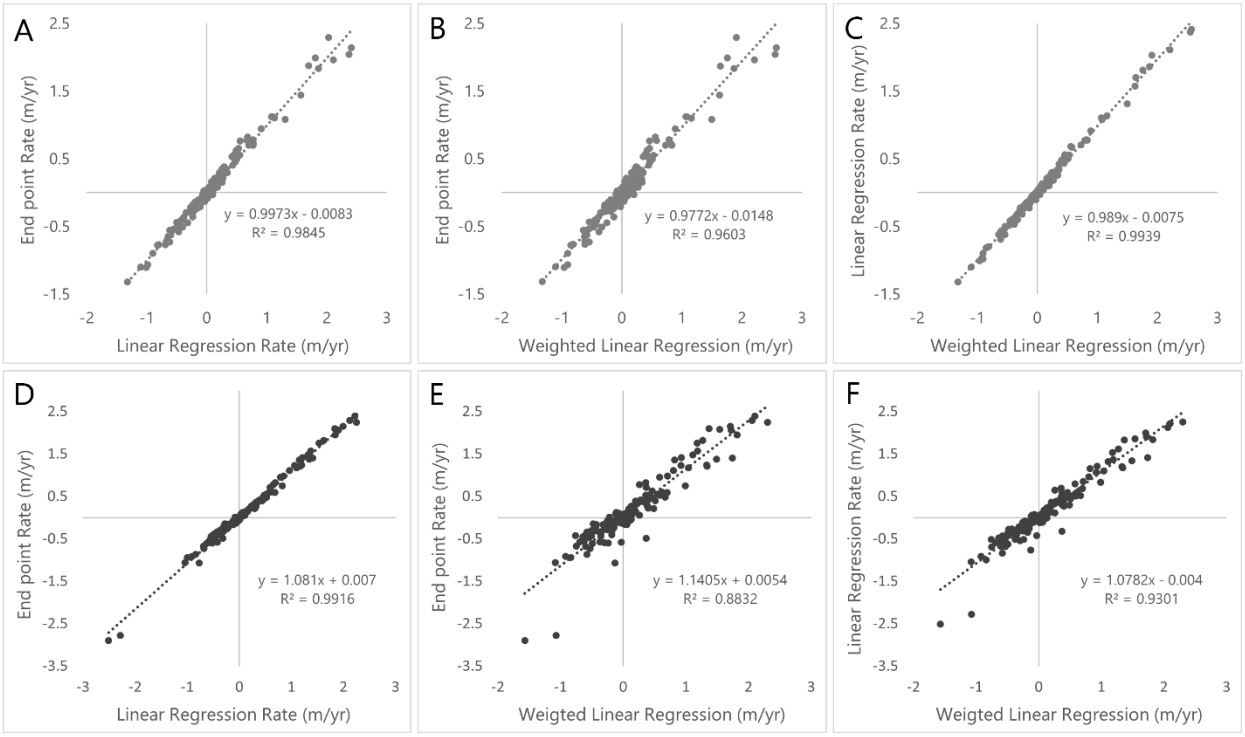

Annex II

Cost-distance results for the 1-year return period. The darker colors indicate closer distance from the flooding source. A) Present scenario. B) 2050 scenario. C) 2050 scenario including the shoreline retreat of the eroding areas. D) 2100 scenario.

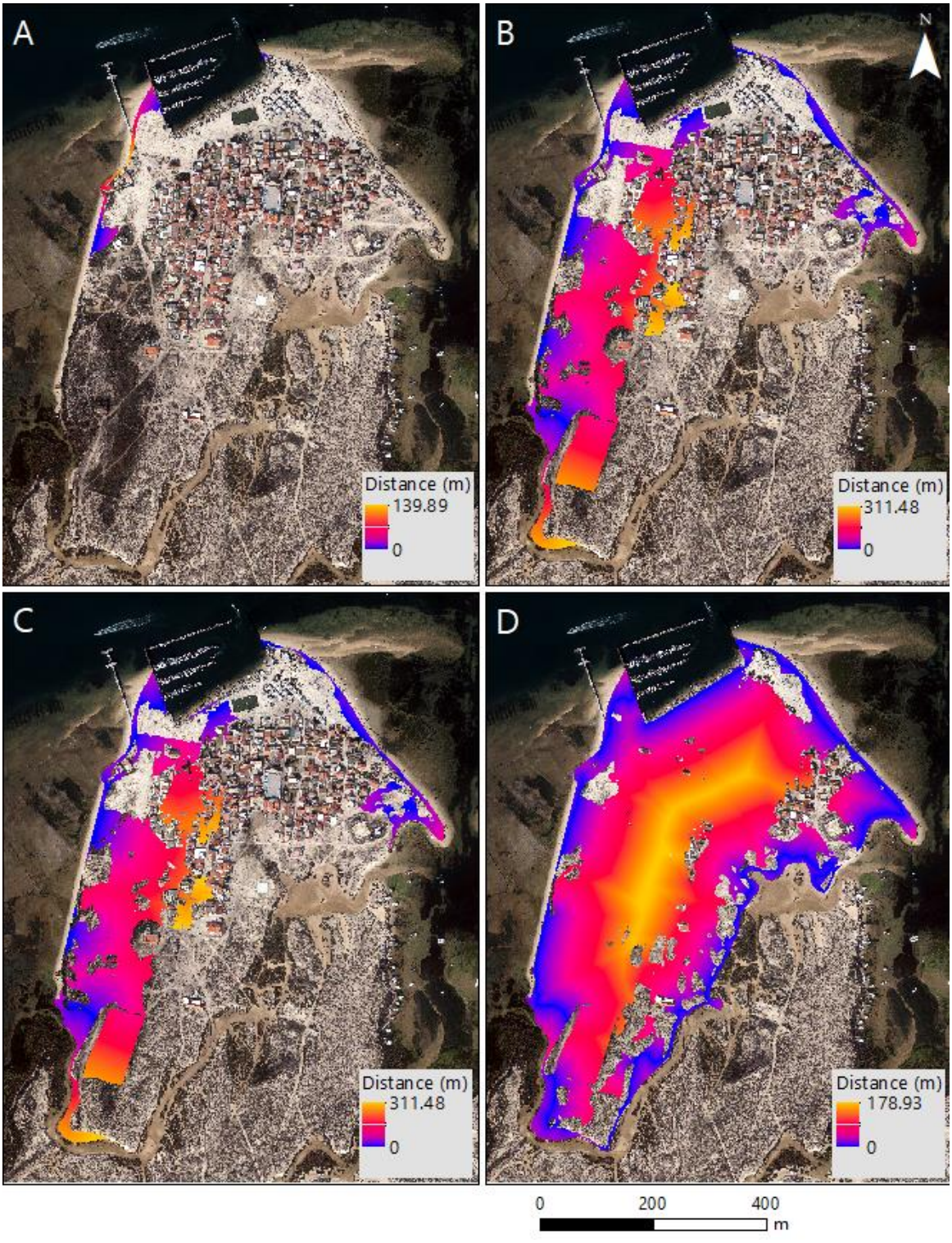

Annex III

Cost-distance results for the 100-year return period. The darker colors indicate closer distance from the flooding source. A) Present scenario. B) 2050 scenario. C) 2050 scenario including the shoreline retreat of the eroding areas. D) 2100 scenario.